Azobenzene Functionalized Block Copolymers for Switchable Drug Delivery Systems

By

CHAUDHARY OMER JAVED

Supervised by

DR. NASIR M. AHMAD

Submitted to the Department of Materials Engineering
School of Chemical & Materials Engineering (SCME),
in partial fulfillment of requirements for the degree of Masters in
Materials and Surface Engineering

National University of Sciences and Technology
Islamabad, Pakistan
October, 2009

IN THE NAME OF ALLAH, MOST GRACIOUS, MOST MERCIFUL

… whoever has fear of God – He will give him a way out and provide for him from where he does not expect. Whoever puts his trust in God – He will be enough for him

(Surat al-Talaq: 2-3)

DEDICATION

To

My Father, Mr. Ch. Arshad Javed

My Mother, Mrs. Mumtaz Begum (late)

And

My Wife, Mrs. Afshan Urooj

whose prayers, support and

encouragement help me in every moment

ABSTRACT

Recent progress in the design and development of self-assembled stimuli-responsive azobenzene block copolymer (BCP) has stimulated researcher to explore their applications in diverse areas including biomedicals such as drug delivery. For this purpose, development of novel materials of responsive functionalities (light- and/or pH) are highly desirable and allow the programmable control on their properties, functions or morphology. To make light a truly appealing and viable stimulus for controlled BCP self-assembly for applications in switchable therapeutic drug delivery, much works remain to be done. The design and synthesis of photo-controllable, and biocompatible self-assembly BCP is vital for future progress in this area. Considering this, main objective of the current research work was to carry out the synthesis of a series of azobenzene based block copolymers functionalized with azobenzene chromophores monomer for optical applications, and *tert*-butyl acrylate monomer for introducing the self-assembly character via its hydrolysis into acrylic acid. The most startling characteristic of the azobenzene is their highly efficient and fully reversible photo-isomerization from the trans to cis form, and therefore polymeric materials incorporating these chromophores present light-switchable properties. The photoisomerization is accompanied by the polar, structural, and optical changes. This photochemically cleaned isomerization can be controlled locally in a well defined manner.

Considering above, diblock copolymers composed of monomers of (*tert*-butyl acrylate) and a side-chain azobenzene-containing monomer, 4-[2-(4-nitrophenyl)diazenyl]phenyl ester (NDP monomer) were prepared using controlled living radica polymerization technique of atom-transfer radical polymerization (ATRP). Experimental strategy involved the synthesis of NDP monomer. For this purpose, acryloyl chloride monomer was synthesized by carrying reaction between acrylic acid and benzoyl chloride. The azo dye of 4-[2-(4-nitrophenyl)diazenyl]phenol (NDP) was prepared by the diazonium salt followed by its reaction with acryloyl chloride by Schotten-Bauman reaction to synthesize NDP monomer functionalized with azobenzene chromophores. The prepared monomer was characterized using infra-red (IR) spectroscopy and NMR spectroscopy to determine its structure. UV-visible absorption

spectroscopy was used to determine the λ_{max}. Broad absorption spectrum was observed with λ_{max} value of 340 nm. The prepared NDP monomer was used to prepare diblock copolymers of P(t-BA-block-NDP) of varying molar masses and degree of polymerization. First, four individual blocks copolymers composed of *tert*-butyl acrylates were synthesized by ATRP to obtain macroinitiator of target degree of polymerization of 20, 45, 70 and 100. Gel permeation chromatography (GPC) was used to determine the molar masses and molar mass distribution of the prepared blocks. The experimentally determined degree of polymerization using GPC found to be 224, 44, 74, 119, and thus exhibited good agreement with the targeted values. Furthermore, the synthesized block copolymers found to be of narrow molar mass distribution (MMD) with values varying between 1.13-1.20. ATRP of the prepared macroinitiators of *tert*-butyl acrylates were then further carried out by carrying its reaction with NDP monomer to synthesize diblock copolymers of P(t-BA-block-NDP). The formation of diblock copolymers were confirmed by the GPC analysis as indicated by a single GPC peak and increase in the molar masses. The degree of polymerization of the NDP monomers were determined to be similar with values in between 40-46, and the MWD values of around 1.25.

ACKNOWLEDGMENTS

I would like to start by acknowledging and thanking my research advisor, Dr. Nasir M. Ahmad. He has provided me with continuous support and guidance. Through his positive feedbacknad critique he helped me develop scientific, communicationm and personal skills that I am sure I will be using for the rest of my professional life.

I would like to thank Mr. Fazal Elahi, Director General SCME, Dr. Muhammad Bilal Khan, Dean and Director Projects SCME, Dr. Amir Azam Khan, HOD Department of Materials Engineering SCME and Dr. Khairuddin Sanaullah, HOD Department of Chemcial Engineering SCME, for their efforts in providing a motivated and friendly environment, and also arranged for lab facilities and chemicals.

I would also like to thank Mr Syed Junaid Ali for providing help in the laboratory. Thanks to Mr Hassan and Mr. Asif for creating a wonderful lab environment. Finally I also like to thank Dr. Muhammad Ilyas Sarwar (Dept. of Chemistry, Quaid-i-Azam University, Islamabad) for valuable guidance, for providing NMR, UV-Vis facilities and also lab facilities for synthesis. Research students at Dept. of Chemistry, Quaid-i-Azam University also helped me in laboratory experimentation specially Mr. Sajjad, Mr. Rizwan, Mr. Sultan, Mr. Zafar Iqbal and Mr. Waqas. Without the contribution of all above this research work was not possible.

Finally I would like to say my special thanks to my wife, for her encouragement, and patience during all my research work.

TABLE OF CONTENTS

LIST OF TABLES

LIST OF FIGURES

CHAPTER 1: LITERATURE REVIEW

1 INTRODUCTION

Synthetic and naturally occurring polymers are important materials, and exhibit a large range of properties and play an important function in everyday life. Naturally occurring polymers are proteins, DNA, carbohydrates etc. Now a days synthetic polymers are finding increasing applications in all fields. The polymeric materials are now being used as pipes, tanks, packing materials, insulation, adhesives, matrix for composites, in many biomaterials, especially heart valve replacements and blood vessels, clothing, floor coverings and these days in medicines as drug delivery systems.

The properties of polymers depend on the monomers (repeat units), degree of branching, chain length and monomer arrangement in polymers. Considering the composition, a homopolymer contain one type of monomer repeats but in a copolymer two or more monomeric species are present. Monomers within a copolymer can be organized along the backbone in a variety of ways to achieve various structure and properties such as given below.

a) **Random copolymers** have monomer types arranged in a chain without any order.
b) **Alternating copolymers** possess regularly alternating monomer residues.
c) **Block copolymers** have two or more homopolymer subunits linked by covalent bonds. Polymers with two or three blocks of two distinct chemical species.
d) **Graft copolymers** contain side chains that have a different composition or configuration than the main chain.

Among the various copolymers, block copolymers have attracted lot of attention in recent years because of their unique chracterstics such as self-assembly. A brief review about the chracterstics of these polymers is outlined below.

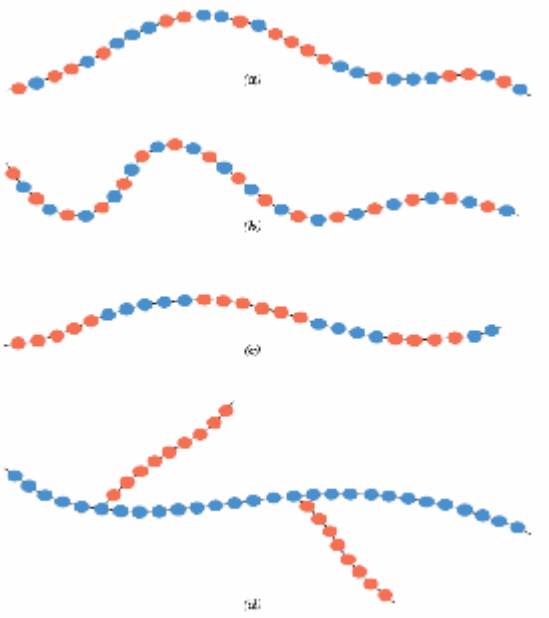

Figure 1.1 Schematic representation of the structure of the copolymers consists of two monomers.

1.1 BLOCK COPOLYMERS

A block copolymer molecule contains two or more polymer chains attached at their ends via covalent bonds. Depending on the number and arrangement of polymer blocks, block copolymers can be a di-block, tri-block, multi-block, cyclic-block, star-block and so on.

Most commonly used notation for the block copolymers is type of A-*b*-B, it denotes a di-block copolymer of polymer A and polymer B. Sometimes the *b* is replaced by the full term block. For example, PS-b-PMMA is short for polystyrene-b-poly(methyl methacrylate) and is made by first polymerizing styrene, and then subsequently polymerizing MMA from the reactive end of the polystyrene chains. This polymer is a "di-block copolymer" because it contains two different chemical blocks.

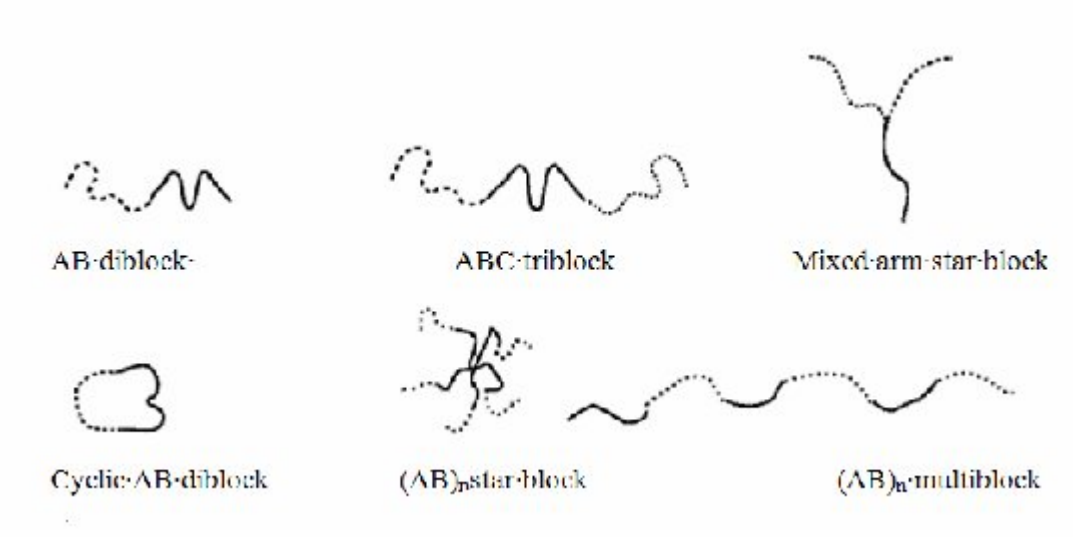

Figure 1.2 Schematics of block copolymer architectures

1.2 SYNTHESIS OF BLOCK COPOLYMERS

Block copolymers are synthesized by using living polymerization techniques also called controlled polymerization techniques. Living polymerization are actually addition polymerization in which premature chain termination is avoided, therefore polymer chains grow with a constant rate having very low polydispersity index. Using living polymerization block copolymers can be synthesized in stages, each stage involving a different monomer. Predetermined molar masses and control over end groups are additional advantages of living polymerizations.

The first living polymerization to synthesize block copolymer was living anionic polymerization. Other important polymerization techniques used to synthesize block copolymers are controlled radical polymerizations (CRP), Ring opening metathesis polymerization (ROMP), Living cationic polymerization and recently developed Chain shuttling polymerization.

1.2.1 LIVING ANIONIC POLYMERIZATION

Anionic polymerization is the most widely employed method for the synthesis of block copolymers. Michael Szwarc was first to use anionic polymerization for the synthesis of block copolymer in 1956 [1]. He synthesized block copolymers of styrene. The method of anionic polymerization has been used industrially for production of block copolymers of styrene and butadiene.

Living anionic polymerization is of wide scope as it can be used with a variety of monomers such as styrenes, dienes, methacrylate, vinyl pyridines, epoxides, cyclic siloxanes, lectones, acrylonitrile, cyanonitrile, propylene oxide, vinyl ketones, acrolein and isocyanate to name a few.

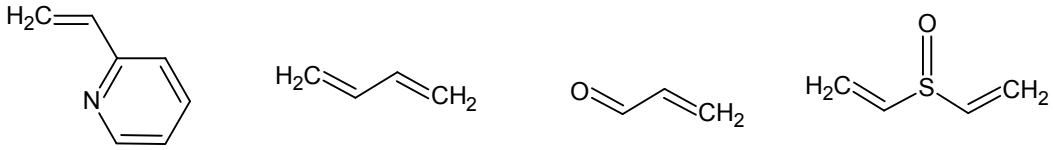

Vinyl pyridine Butadiene acrolein vinyl sulfoxide

Figure 1.3 Few monomers capable of undergoing anionic polymerization.

Also blocks of predetermined and controlled molecular weights can be prepared with very low polydispersity index. Despite of the advantages the main limitation of this technique is that it requires high purity reagents and high vacuum to avoid accidental termination by impurities and moisture.

Initiation can occur through carbanion formation, either by electron transfer from alkali metals or through strong neucleophiles/anions [2]

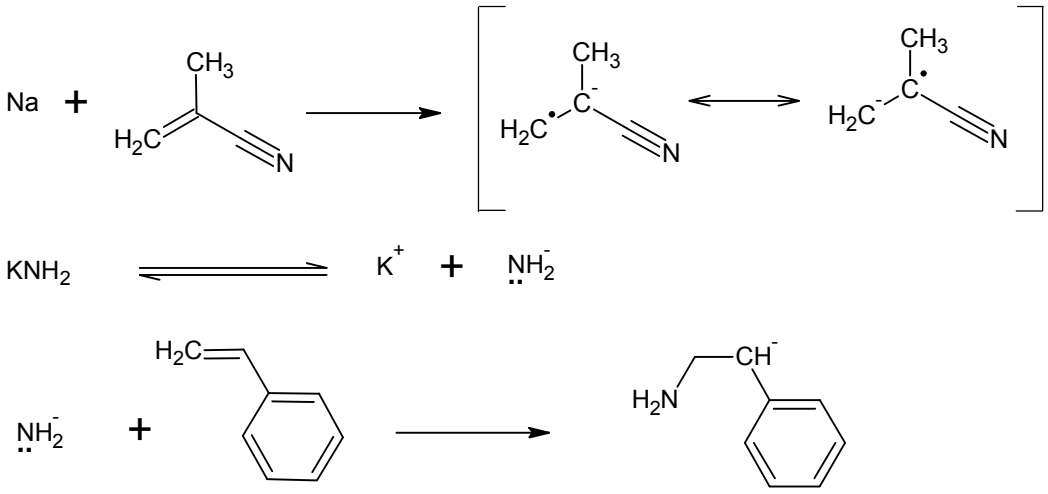

Figure 1.4 Mechanisms of initiation in Living anionic polymerizations.

Once carbanion is produced the reaction propagates with high velocity. But carbanion is only stable at low temperatures at higher temperatures, side reactions are dominant. Polymerization continues until the consumption of all monomers. As reaction is fast so all chains start and propagate simultaneously, resulting in very low

polydispersity index. Also the number of chains is equal to the number of initiator molecules involved, thus degree of polymerization is predetermined.

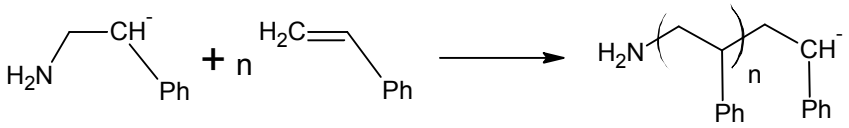

Figure 1.5 Mechanism of propagation in Living anionic polymerization.

Living anionic polymerization lacks a formal termination step, so termination can be unintentional quenching due to impurities (e.g. oxygen, carbon dioxide, water) or international by adding water or alcohol. But termination can also occur when some specie in the reaction mixture acts as Bronsted acid and result in chain transfer.

The choice of solvent and initiator depends on the reactivity of monomer and also on the stability of carbanion intermediate. Mostly aprotic solvents are used and anionic polymerization can performed in solution, suspension and emulsion.

Due to precise control offered, living anionic polymerization have not only being used for the synthesis of di-block and tri-block copolymers but also used in the synthesis of mixed arm stars [3,4] and ring shaped (cyclic) block copolymers [5]. Another added advantage of anionic polymerization is the ability to produce desired functional group at the end of the chain [6].

1.2.2 LIVING RADICAL POLYMERIZATION

In ionic polymerization the growing chains are mutually repulsive but in case of radical polymerization radical combination and disproportionation occurs. Recently, development of living radical polymerization or controlled radical polymerization (CRP) techniques, such as stable free radical polymerization (SFRP), Atom transfer radical polymerization (ATRP) and reversible addition fragmentation transfer (RAFT), leads to the synthesis of new block copolymers. In all living radical polymerizations the equilibrium between dormant chains (those reversible terminated with the free radical) and active chains (those with a radical capable of addition to monomer) is designed to favor the dormant state. Such an equilibrium not only minimized the probability of the radical bimolecular termination but also provides an equal opportunity for all living and dormant chains to propagate via the frequent interconversion between the active and dormant species, hence all chains grow uniformly. Although termination reactions of the growing radical chains are reduced but still around 10% of the growing radicals are

terminated during the polymerization [7]**.** Following are the some major types of controlled racial polymerizations.

1.2.2.1 STABLE FREE RADICAL POLYMERIZATION (SFRP)

Stable free racial polymerization is also called nitroxide-mediated polymerization (NMP). In Stable free racial polymerization a stable radical is introduced which acts as radical scavenger. Coupling of stable free radical with the polymeric radical is reversible in such a way that the propagation radical concentration is limited to the levels that allow controlled polymerization.

Initially TEMPO was used as stable free radical. Due to a few problems associated with TEMPO several new nitroxides were introduced to broad the scope of SFRP [8].

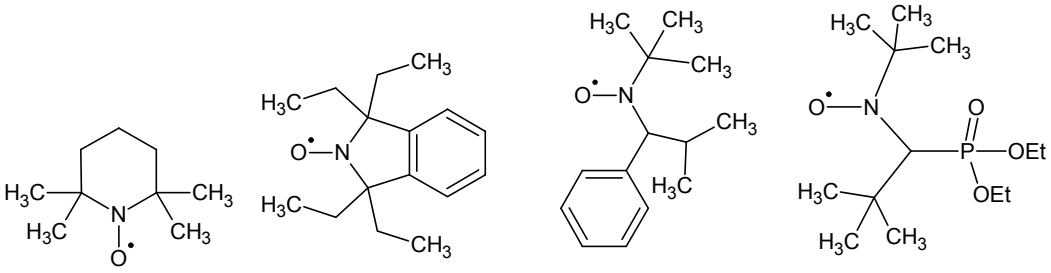

Figures 1.6 Structure of a few stable nitroxide radicals.

1.2.2.2 ATOM TRANSFER RADICAL POLYMERIZATION (ATRP)

Atom transfer radical polymerization was developed by Krzysztof Matyjaszewski in 1995 [9]. It involves the chain initiation of free radical polymerization by an organic halide (initiator) in the presence of a metal halide (catalyst). The metal abstracts halide from the organic halide to generate a radical which then starts free radical polymerization. During propagation, the radical on the active chain terminus is reversibly terminated (with the halide) by reacting with the catalyst in its higher oxidation state. Therefore, the redox processes give rise to equilibrium between dormant (Polymer-Halide) and active (Polymer-Radical) chains. The equilibrium favors the dormant state, so that radical concentration remains lower to avoid bimolecular coupling. Such polymerizations require temperatures of about 60-120°C. ATRP methods are advantageous due to ease of preparation, and commercially available and less expensive catalysts, ligands and initiators.

The catalyst is one of the most important components of ATRP as it determines the equilibrium constant between the active and dormant species. Several metal halides have been used as catalyst but mostly copper halides are used due to greater control in polymerizations with many monomers. One of the main problem with metal halides is a low solubility in organic solvents, which results in limited availability of the catalyst. To increase the solubility of catalyst, a ligand is added to form complex with the catalyst. But sometimes monomer is also capable of forming complex with the catalyst thus lowering polymerization rates [10], therefore in such cases a stronger binding agent, such as the tridentate N,N,N',N",N"-pentamethyldiethylenetriamine (PMDETA) is used.

Block copolymers can be prepared via sequential controlled radical polymerization, or via controlled radical polymerization using macroinitiators. The first method is the simple addition of a second monomer into the reaction medium after near-complete conversion of the first monomer. The second method involves the isolation and the purification of the first polymer, then using it as a macroinitiator. Although the first method is easy to carry out, the second block may produce a random copolymer because complete conversion in the controlled radical system is impossible, and loss of the terminal bromine at the end of polymer chain may occur after many steps of redox. In order to avoid the troublesome separation of block copolymers from the homopolymer, the ATRP is generally stopped at lower conversion of the first monomer polymerization in order to ensure one bromine group at each end of the polymer chain.

The number of growing polymer chains is determined by the initiator. The faster the initiation and fewer terminations and transfers, the more consistent will be the number of propagating chains, leading to narrow molecular weight distributions. Normally those organic halides, which are similar in the organic framework as the propagating radical, are chosen as initiators. Normally alkyl bromides and alkyl chlorides are chosen as initiator due to control over molecular weight. Alkyl bromides are more reactive then alkyl chlorides.

Monomers that are used with ATRP are those which have substituents that can stabilize the propagating radicals. Mostly ATRP have been done with styrenes, acrylates and methacrylates. Block copolymers of methacrylamide, acrylonitrile. Vinyl pyridine have also been synthesized.

ATRP reactions are tolerant to many functional groups like, allyl, amino, epoxy, hydroxyl and vinyl groups present in either the monomer or the initiator [11]. ATRP cannot be used to polymerize some functional monomers, especially monomers having

acidic groups, such as acrylic acid or methacrylic acid. The protection-deprotection technique is an important method to synthesize amphiphilic block copolymers containing such blocks [12].

Using ATRP several type of block copolymers have been synthesized but mostly AB and ABA type block copolymers have been synthesized

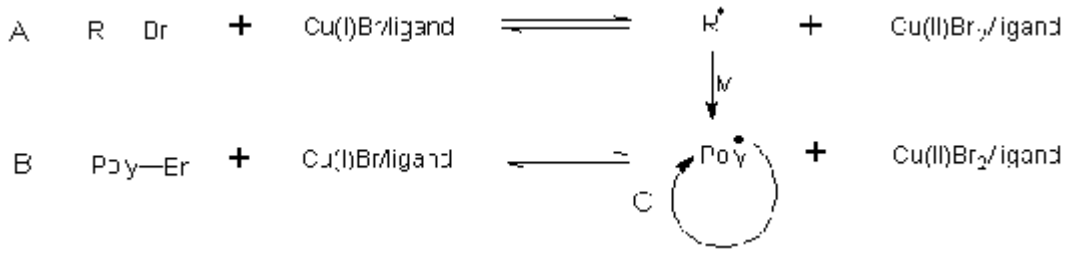

Where A = Initiation, B = Equilibrium with dormant specie and C = Propagation

Figure 1.7 Mechanism of Atom Transfer Radical Polymerization

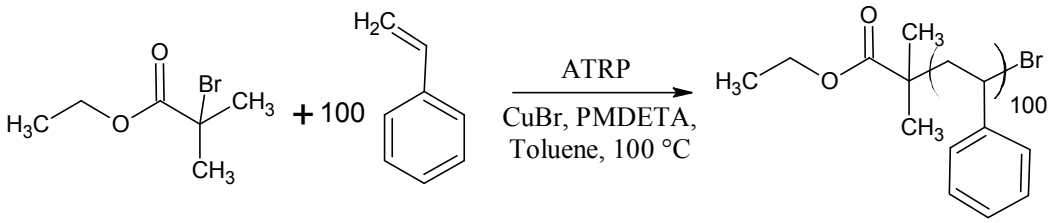

Figures 1.8 Atom Transfer Radical Polymerization of Polystyrene

1.2.2.3 REVERSIBLE ADDITION FRAGMENTATION CHAIN TRANSFER (RAFT) POLYMERIZATION

RAFT was discovered in 1998 by Moad and coworkers at CSIRO [13]. This technique is exceptionally versatile in providing polymers with predetermined molecular weights and narrow polydispersity. Implementing RAFT technique is very simple. By just introduction of a suitable chain transfer agent, known as a RAFT agent, into a conventional free radical polymerization reaction, gives the polymerization living characteristics. Reaction must be performed in the absence of oxygen, which terminates propagation.

The RAFT agent is the main specie in RAFT polymerization. Normally RAFT agents are dithio compounds. Here initiator generates a free radical which then reacts with a monomer molecule to form the active centre and starts propagating. These propagating polymer chains react rapidly with the transfer agent [S=C(Z)S-R] to form a

polymeric transfer agent [S=C(Z)S-R] in the early stage of polymerization. Fragmentation of this intermediate gives rise to either the original polymer chain or to a new radical which itself is able to form another active centre and leads to a new propagating chain. The S=C(Z)S- moiety is transferred between dormant and active chains, leading to the living character of polymerization. As majority of chains in the target polymer have the S=C(Z)S- group, polymerization of a second monomer can be continued to give a block copolymer.

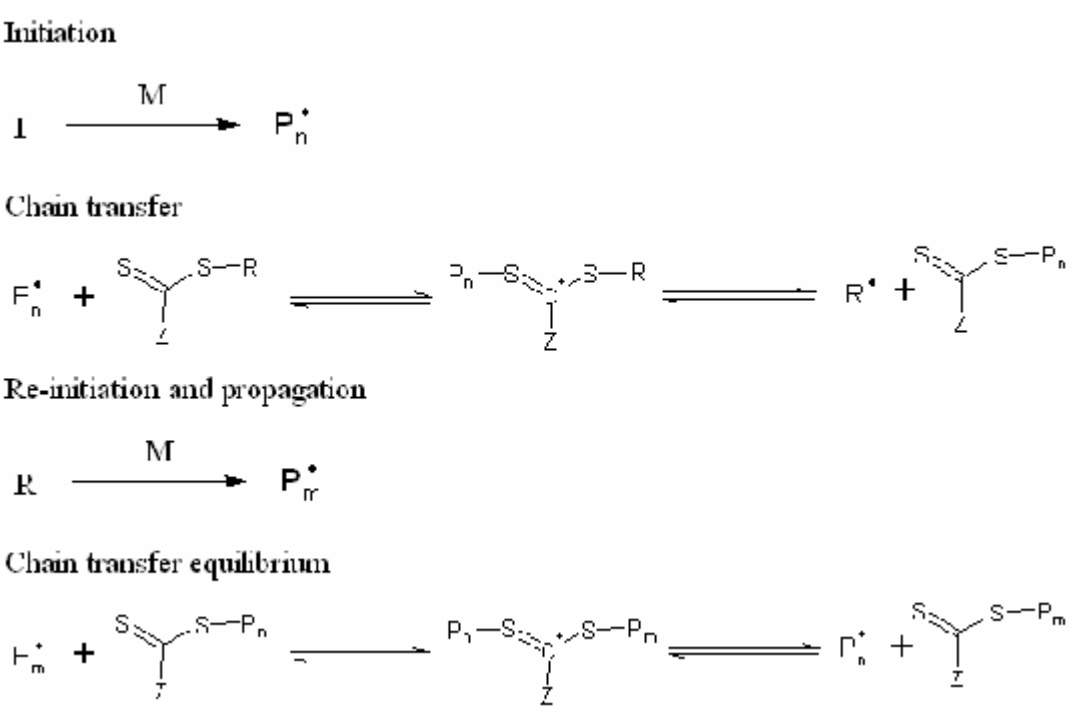

Figure 1.9 Mechanism of Reversible Addition Fragmentation Chain Transfer Polymerization

In principle, one requirement for the formation of a narrow polydispersity. AB block copolymer in a batch polymerization is that the first-formed polymeric thiocarbonyl transfer agent (S=C(Z)S-A) should have a high transfer constant in the subsequent polymerization step to give the B block. This requires that the leaving group of propagating radical A• is comparable to or better than that of the propagating radical B• under the conditions of the reaction. Therefore, when preparing a block copolymer, the polymerization of the monomer with the higher transfer constant should be carried out first. For example, macrotransfer agent PMMA-SC(Z)S is prepared first by the

polymerization of MMA in the RAFT polymerization condition, and then used in the RAFT polymerization of the second monomer, such as St or MA. Diblock copolymers PMMA-b-PSt or PMMA-b-PMA with well-controlled MW and narrow MWD were then obtained.

In the RAFT process, the total number of chains formed will be equal to (or less than) the number of moles of dithio compound employed plus the number of moles of initiator-derived radicals generated during the course of the polymerization. In block copolymer synthesis, these additional initiator-derived chains are a source of homopolymer impurity. The level of impurities can be controlled by appropriate selection of the reaction conditions. To reduce impurities, it is desirable to use as low a concentration of initiator as practicable, and to choose solvents and initiators that give minimal chain transfer. Similar to conventional radical polymerization, the rate of RAFT polymerization is determined by the initiator concentration. In practice, it is usually not difficult to achieve block copolymers with no detectable homopolymer impurity (<5 %), while still achieving an acceptable rate of polymerization. RAFT polymerization can be performed in bulk, in solution or in an emulsion [14]. RAFT has been employd for the synthesis of AB, ABA and ABC type block copolymers.

1.2.3 OTHER METHODS

Cationic polymerization has also been developed but it is successful with only few monomers and needs careful optimization in order to obtain polymers with controlled molecular weights. The most synthesized blocks are that of vinyl ethers, as these are easiest to synthesize by such methods [15]. Sometimes cationic polymerization is successful with specific monomers, while other polymerization techniques not.

Coupling reactions are also used to synthesize block copolymers. This is the only method to form a block copolymer when sequential polymerizations methods are not possible. But the main draw back of coupling reactions in the preparation of block copolymers is that a purification step is required to obtain pure block copolymer because unreacted precursor polymer is always present in the crude product. Coupling reactions are most commonly used when both monomers cannot undergo polymerization through similar mechanism. Hence, mostly triblock colpolymers and mixed arm starblock copolymers can be prepared using coupling reactions of already synthesized polymer chains. Chlorosilanes are mostly used as coupling agents. As an example, PCHD-PS three arm stars were prepared by linking the corresponding diblock with TCMS [16].

There have been numerous examples of transformation reactions that either preformed macroinitiators or different polymerization techniques with the living polymerizations of various monomers. The majority of the work reporting on use of commercially available macroinitiators to prepare block copolymers describes the use of macroinitiators derived from poly(ethylene glycol) (PEG) which can be used to produce amphiphilic block copolymers [17].

Many polymerization techniques have been combined with CRP through site transformation of the active species. These include non-living techniques like condensation and conventional free radical processes or living methods like anionic, cationic, and ring-opening polymerizations, as well as others.

Non-living polymerization techniques can be combined with CRP methods to produce block copolymers. The first example of transforming a hydroxy functionality into an ATRP initiator was demonstrated by Gaynor and Matyjaszewski [18].

Carbocationically prepared α,ω-difunctional polyisobutylene (pIB), possessing a terminal chlorine functionality was capped with several St units, then used as the macroinitiator for the ATRP of St, MMA, MA, and isobornyl acrylate (IA) using the CuCl/dNbpy catalyst system, as reported by Coca and Matyjaszewski [19]

Living anionic polymerization has also been used to prepare macroinitiators for subsequent chain extension to form block copolymers using CRP methods. There are several examples in the literature of using anionically prepared pBD to initiate either ATRP or nitroxide-meditated polymerizations. Priddy et al. used an epoxy-functional TEMPO moiety to terminate the living anionic polymerization of BD, which was then employed as an initiator for the polymerization with St to create high-impact pSt in situ [20].

Poly(tetrahydrofuran), pTHF, prepared through living cationic ring-opening polymerization (CROP), was reacted with sodium OTEMPO to produce a counter radical for polymerization of St to form block copolymers, by Yoshida and Sugita [21].

Matyjaszewski et al. demonstrated that living ring opening metathesis polymerization (ROMP) could also be combined with ATRP to produce novel block copolymers [22]. ROMP of norbornene (NB) and dicyclopentadiene (CPD) were performed using an Mo-alkylidene complex, followed by reaction with *p*-(bromomethyl) benzaldehyde to generate a benzyl bromide terminated polymer capable of being used as a macroinitiator for ATRP.

Recently a new technique named “Chain Shuttling Polymerization” is developed for the synthesis of block copolymers. Chain Shuttling Polymerization is a dual-catalyst method for producing block copolymers with alternating or variable tacticity. The desired effect of this method is to generate hybrid polymers that bear the properties of both polymer chains, such as a high melting point accompanied by high elasticity. It is a relatively new method, the first instance of its use being reported by Arriola et al. in May of 2006 [23].

1.3 PHASE BEHAVIOUR OF BLOCK COPOLYMERS

1.3.1 BULK

One of the well-known features of polymers is their immiscibility, which occurs as a result of entropic reasons. Practically this means that the mixing of two different polymers, with dissimilar physicochemical characteristics, results in macroscopic phase separation. Block copolymers of an AB type, in which two chemically different blocks are linked together via covalent bonding, also exhibit phase separation, but on the smaller, microscopic scale [24]. This microscopic separation is possible through the simultaneous existence of two opposite forces in the system: long-range repulsive and short-range attractive forces. Incompatibility of the two blocks causes long-range repulsive interactions whereas the covalent bond, which links the blocks together, is responsible for the short-range attractive force (Figure 1.10)

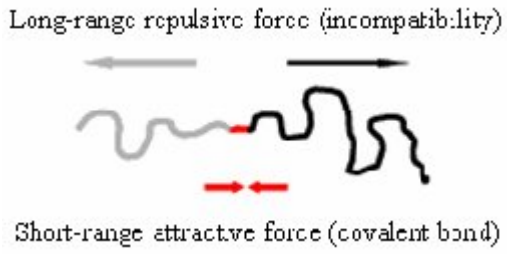

Figure 1.10 Schematic representation of two simultaneously present interactions leading to the self-organisation of block copolymers.

The most commonly observed bulk morphologies of microphase-separated block copolymers are ordered continuous phases such as bcc-packed spheres *(BCC)*, hexagonally ordered cylinders *(HEX)*, lamellae *(LAM)*, and bicontinuous *gyroid* structures (Figure 1.11).

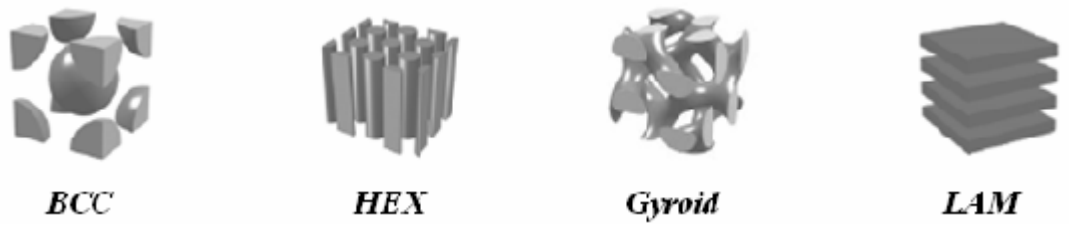

Figure 1.11 Commonly observed bulk morphologies of microphase-separated block copolymers.

The phase behaviour of block copolymer melts is, to a first approximation, represented in a morphology diagram in terms of χN and f [25]. Here f is the volume fraction of one block and χ is the Flory–Huggins interaction parameter, which is inversely proportional to temperature, which reflects the interaction energy between different segments. The configurational entropy contribution to the Gibbs energy is proportional to N, the degree of polymerization. When the product χN exceeds a critical value, $(\chi N)_{ODT}$ (ODT = order–disorder transition) the block copolymer microphase separates into a periodically ordered structure, with a lengthscale ~5-500nm. The structure that is formed depends on the copolymer architecture and composition [25]. For diblock copolymers, a lamellar (lam) phase is observed for symmetric diblocks (f =0.5), whereas more asymmetric diblocks form hexagonal-packed cylinder (hex) or body-centred cubic (bcc) spherical structures. A complex bicontinuous cubic gyroid (gyr) phase has also been identified [26] for block copolymers between the lam and hex phases near the ODT. The ODT in block copolymers can be located via a number of methods – from discontinuities in the dynamic shear modulus [27] or small-angle scattering peak shape [28] or from calorimetry measurements [29]. The preparation method can also have a dramatic influence on the apparent morphology, for example whether solvent casting or melt processing is performed.

To establish relationships between different block copolymer phase diagrams and also to facilitate comparison with theory, it is necessary to specify parameters in addition to χN and f. First, asymmetry of the conformation of the copolymer breaks the symmetry of the phase diagram about f =0.5. For AB diblocks, conformational asymmetry is quantified using the ‘‘asymmetry parameter’’ $\varepsilon = (b_A^2/v^A)/(b_B^2/v^B)$ [30], where b^J is the segment length for block J and v^J is the segment volume. Composition fluctuations also modify the phase diagram, and this has been accounted for theoretically via the Ginzburg parameter $N=Nb^6\rho^2$, where ρ is the number density of chains [31]. The

extent of segregation of block copolymers depends on the magnitude of χN. For small χN, close to the order–disorder transition (up to χN = 12 for symmetric diblocks for which χN_{ODT} = 10.495), the composition profile (density of either component) is approximately sinusoidal. This is termed the weak-segregation limit. At much larger values of χN($\chi N \geq 100$), the components are strongly segregated and each domain is almost pure, with a narrow interphase between them. This is the strong-segregation limit.

The first theories for block copolymers were introduced for the strong-segregation limit (SSL) and the essential physical principles underlying phase behaviour in the SSL were established in the early 1970s [25]. Most notably, Helfand and coworkers [32] developed the self-consistent field (SCF) theory, this permitting the calculation of free energies, composition profiles and chain conformations. In the SCF theory, the external mean fields acting on a polymer chain are calculated self-consistently with the composition profile. The theory of Leibler [33] describes block copolymers in the weak-segregation limit. It employs a Landau–Ginzburg approach to analyse the free energy, which is expanded with reference to the average composition profile. The free-energy coefficients are computed within the random-phase approximation. Weak-segregation limit theory can be extended to allow for thermal-composition fluctuations. This changes the mean-field prediction of a second-order phase transition for a symmetric diblock copolymer to a first-order transition. Fredrickson and Helfand [31] studied this effect for block copolymers and showed that composition fluctuations, incorporated via the renormalization method of Brazovskii, lead to a ‘‘finite-size effect’’, where the phase diagram depends on N. A powerful new method to solve the self-consistent field equations for block copolymers has been applied by Matsen and coworkers [34] to analyse the ordering of many types of block copolymer in bulk and in thin films. The strong- and weak segregation limits are spanned, as well as the intermediate regime where the other methods do not apply. This implementation of SCF theory predicts phase diagrams, and other quantities such as domain spacings, in good agreement with experiment (see Figure 1.12) and represents an impressive state-of-the-art for modelling the ordering of soft materials. Accurate liquid-state theories have also been used to model block copolymer melts [35], although Figure 1.12 Phase diagram for a conformationally symmetric diblock copolymer, calculated using self-consistent mean field theory [34], along with illustrations of the equilibrium morphologies. In the phase diagram, regions of stability of disordered (dis),

lamellar (lam),gyroid (gyr), hexagonal (hex) and body-centred cubic (bcc) phases are indicated. They are hard to implement and consequently the method is often, regrettably, overlooked [25]. Recently, a method has been developed to directly simulate field theories for polymers without introducing approximations such as mean-field approaches, perturbation expansions, etc. [36]. This technique holds much promise for examining the thermodynamics of block copolymers in the limit of low molecular weight where approximate methods such as mean-field theory or renormalization techniques break down.

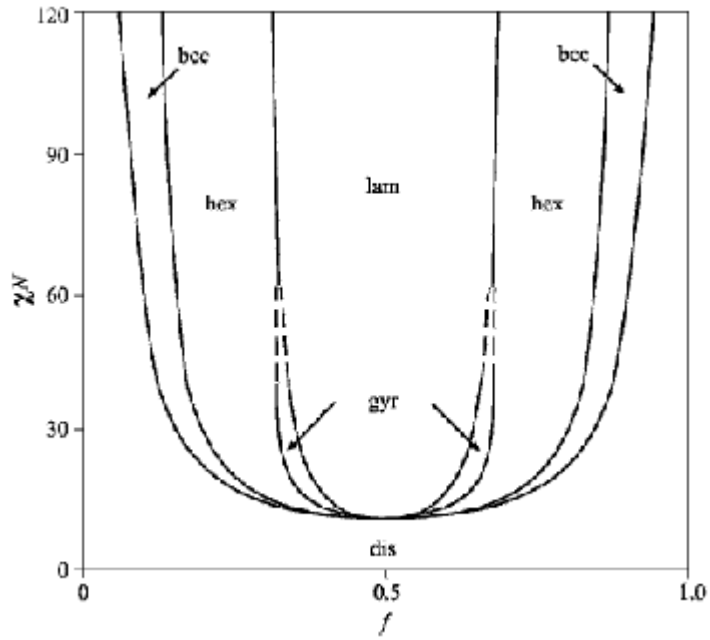

Figure 1.12 Phase diagram for a conformationally symmetric diblock copolymer, calculated using self-consistent mean field theory [34], along with illustrations of the equilibrium morphologies. In the phase diagram, regions of stability of disordered (dis), lamellar (lam), gyroid (gyr), hexagonal (hex) and body-centred cubic (bcc) phases are indicated.

A phase diagram computed using self-consistent mean field theory [34] is shown in Figure 1.12. This shows the generic sequence of phases accessed just below the order–disorder transition temperature for diblock copolymers of different compositions. The features of phase diagrams for particular systems are different in detail, but qualitatively they are similar, and well accounted for by SCF theory.

The phase behaviour of ABC triblocks is much richer than two component diblocks or triblocks, as expected because multiple interaction parameters (χAB, χAC and χBC) result from the presence of a distinct third block.

During processing, block copolymers are subjected to flow. For example, thermoplastic elastomers formed by polystyrene-*b*-polybutadiene-*b*-polystyrene (SBS) triblock copolymers, are moulded by extrusion. This leads to alignment of microphase-separated structures. This was investigated in the early 1970s by Keller and co-workers [37] who obtained transmission electron micrographs from highly oriented specimens of Kraton SBS copolymers following extrusion. Examples are included in Figure 1.13. The application of shear leads to orientation of block copolymer microstructures at sufficiently high shear rates and/or strain amplitudes (in the case of oscillatory shear). Depending on shear conditions and temperature, different orientations of a morphology with respect to the shear plane can be accessed. The ability to generate distinct macroscopic orientation states of block copolymers by shear is important in future applications of block copolymers, where alignment will be important (reinforced composites, optoelectronic materials and separation media). Shear also influences thermodynamics, since the order–disorder transition shifts upwards on increasing shear rate because the ordered phase is stabilized under shear [38].

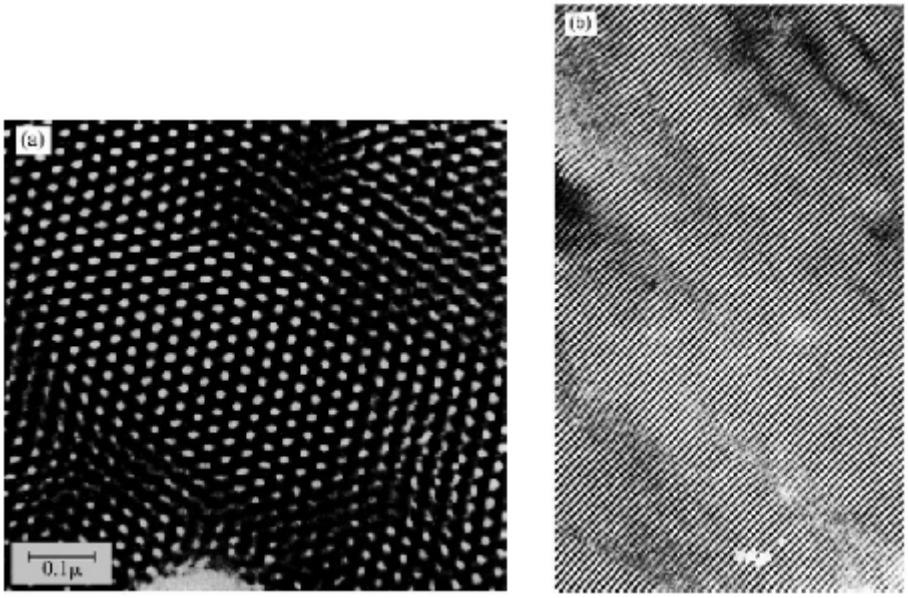

Figure 1.13 TEM micrographs from a hexagonal-packed cylinder structure subjected to flow during high-temperature extrusion. The sample was a PS-PB-PS tribock.

(a) Perpendicular to the extrusion direction, (b) a parallel section.

The main techniques for investigating solid block copolymer microstructures are transmission electron microscopy (TEM) and small-angle X-ray or neutron scattering. TEM provides direct images of the structure, albeit over a small area of the sample. Usually samples are stained using the vapours from a solution of a heavy metal acid (OsO_4 or RuO_4) to increase the contrast for electrons between domains. Small-angle scattering probes the structure over the whole sample volume, giving a diffraction pattern. The positions of the reflections in the diffraction pattern can be indexed to identify the symmetry of the phase [25,37].

1.3.2 BLOCK COPOLYMER FILMS

Microphase separation by block copolymers in thin films has been investigated from several perspectives. First, the physics of self-assembly in confined soft materials can be studied using model block copolymer materials for which reliable mean-field statistical mechanical theories have been developed [39]. Second, interest has expanded due to potential exciting applications that exploit self-organization to fabricate high-density data-storage media [40], to lithographically pattern semiconductors with ultrasmall feature sizes [41] or to prepare ultrafine filters or membranes [42].

Block copolymer films can be prepared by the spin-coating technique, where drops of a solution of the polymer in a volatile organic solvent are deposited on a spinning solid substrate (often silicon wafers are used due to their uniform flatness). The polymer film spreads by centrifugal forces, and the volatile solvent is rapidly driven off. With care, the method can give films with a low surface roughness over areas of square millimetres. The film thickness can be controlled through the spin speed, the concentration of the block copolymer solution or the volatility of the solvent, which also influences the surface roughness. Dip coating is another reliable method for fabricating uniform thin films. Whatever the deposition technique, if the surface energy of the block copolymer is much greater than that of the substrate, dewetting will occur.

In thin films, the lamellae formed by symmetric block copolymers can orient either parallel or perpendicular to the substrate. A number of possible arrangements of the lamellae are possible, depending on the surface energies of the blocks and that of the substrate, and whether the film is confined at one or both surfaces. These are illustrated in Figure 1.14. In the case that a different block preferentially wets the interface with the substrate or air, wetting is asymmetric and a uniform film has a thickness $(n + 1/2)d$. If the initial film thickness is not equal to $(n + 1/2)d$, then islands or holes (quantized steps

of height *d*) form to conserve volume [43]. As well as leading to distinct orientations, confinement of block copolymers can change the thermodynamics of ordering, in particular surface-induced ordering persists above the bulk order–disorder transition [44].

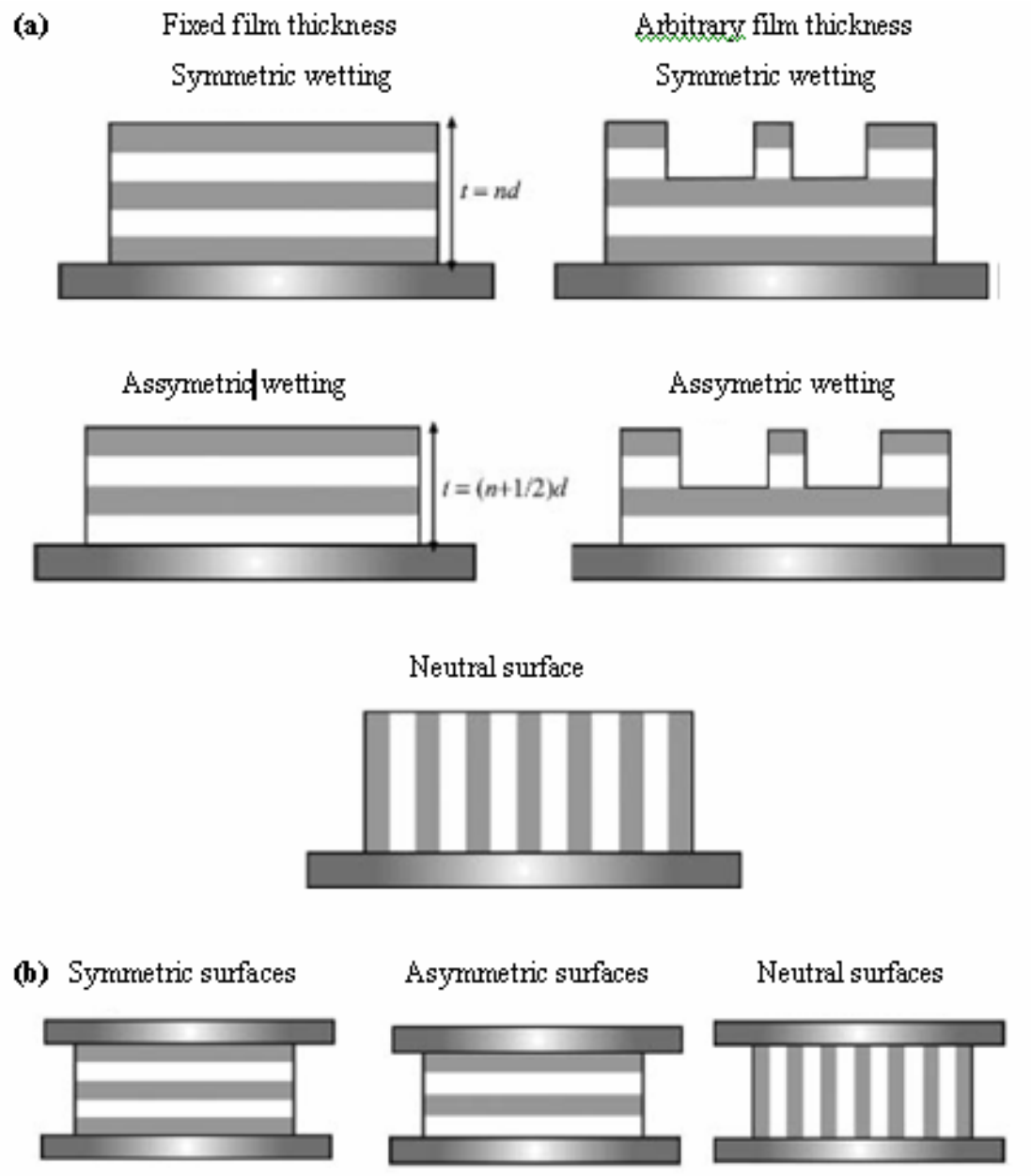

Figure 1.14 Possible configurations of lamellae in block copolymer films. (a) Confined at one surface. (b) Confined at both surfaces.

Asymmetric block copolymers that form hexagonal or cubic-packed spherical morphologies in the bulk, form stripe or circular domain patterns in two dimensions, as illustrated in Figure 1.15. The stripe pattern results from cylinders lying parallel to the substrate, and a circular domain surface pattern occurs when cylinders are oriented perpendicular to the substrate, or for spheres at the surface. Bicontinuous structures cannot exist in two dimensions, therefore the gyroid phase is suppressed in thin films. More complex multiple stripe and multiple circular domain structures can be formed at the surface of ABC triblocks [45].

The morphology of block copolymers on patterned substrates has attracted recent attention. It has been shown that block copolymer stripes are commensurate with striped substrates if the mismatch in the two lengthscales is not too large.

The surface morphology of block copolymer films can be investigated by atomic force microscopy. The ordering perpendicular to the substrate can be probed by secondary ion mass spectroscopy or specular neutron or X-ray reflectivity. Suitably etched or sectioned samples can be examined by transmission electron microscopy. Islands or holes can have dimensions of micrometers, and consequently may be observed using optical microscopy.

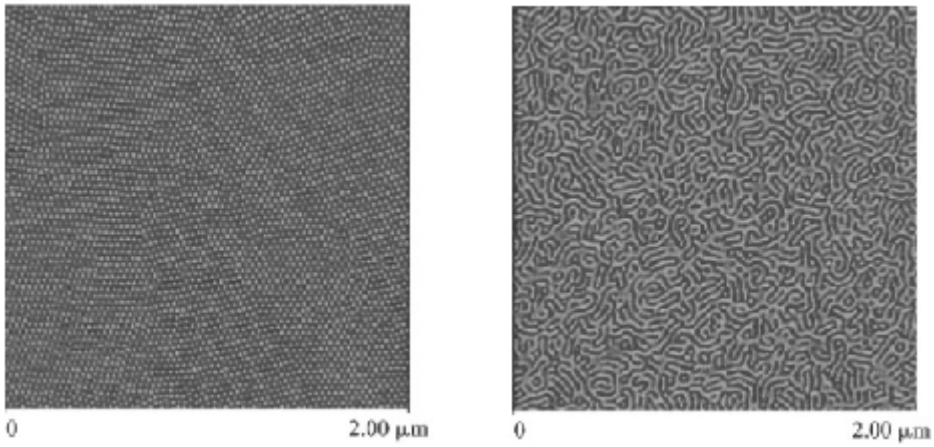

Figure 1.15 Hexagonal and stripe patterns observed via atomic force microscopy (Tapping Mode2). Phase contrast images of (a) polystyrene-b-poly(ethylene-co-butylene)-b-polystyrene Kraton G1657, (b) Kraton G1650 [46].

Theory for block copolymer films has largely focused on the ordering of lamellae as a function of film thickness. Many studies have used brush theories for block

copolymers in the strong-segregation limit [47], although selfconsistent field theory has also been employed [39]. Theory for weakly segregated block copolymers has been applied to analyse surface-induced order above and below the bulk order–disorder transition of a lamellar phase [48] and surface-induced layering in a hexagonal block copolymer film [49].

1.3.3 BLOCK COPOLYMERS IN SOLUTION

In a solvent, block copolymer phase behaviour is controlled by the interaction between the segments of the polymers and the solvent molecules as well as the interaction between the segments of the two blocks. If the solvent is unfavourable for one block this can lead to micelle formation in dilute solution. The phase behaviour of concentrated solutions can be mapped onto that of block copolymer melts [50]. Lamellar, hexagonal-packed cylinder, micellar cubic and bicontinuous cubic structures have all been observed (these are all lyotropic liquid-crystal phases, similar to those observed for nonionic surfactants). This is illustrated by representative phase diagrams for Pluronic triblocks in Figure 1.16.

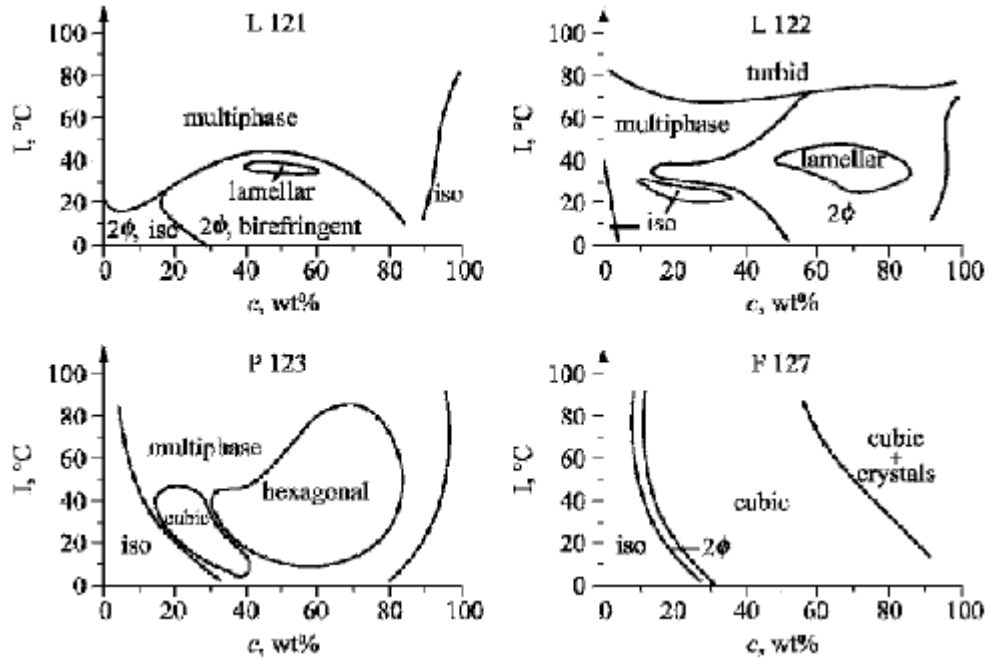

Figure 1.16 Phase diagrams in water of $E_mP_nE_m$ (E=polyoxyethylene, P=polyoxypropylene) Pluronics with n=69 and m=4 (Pluronic L121), m=11 (Pluronic L122), m=20 (Pluronic P123) and m=99 (Pluronic F127) [51].

The main classes of block copolymer examined in solution are those based on polyoxyethylene, which is water soluble and is the basis of most amphiphilic block copolymers, and styrenic block copolymers in organic solvents. Polyoxyethylene-based block copolymers include those of polyoxyethylene (E) with polyoxypropylene (P), especially EPE triblocks (commercial name: Pluronic or Synperonic), which are widely used commercially as surfactants in detergents and personal care products**,** and also in pharmaceutical applications, especially drug delivery [52].

Like surfactants, block copolymers form micelles above a critical concentration. The critical micelle concentration can be located by a variety of techniques, the most commonly used being surface tensiometry where the cmc is located as the point at which the surface tension becomes essentially independent of concentration. The primary methods to determine micelle size and shape are light scattering and small-angle X-ray and neutron scattering. The thermodynamic radius (from the thermodynamic volume, which is one eighth of the excluded volume) of micelles can be obtained from static light scattering experiments by fitting the Debye function to the Carnahan–Starling equation for hard spheres. This procedure can be used in place of Zimm plots when the angular dependence of the scattered intensity is weak, which is usually the case for block copolymer micelles, which are much smaller than the wavelength of light [53]. Static light scattering also provides the association number (from the micellar mass) and the second virial coefficient [25,53]. Dynamic light scattering provides the hydrodynamic radius from the mode corresponding to micellar diffusion obtained from the intensity distribution of relaxation times. The Stokes–Einstein equation can then be used to calculate the hydrodynamic radius from the diffusion coefficient [25,53]. Smallangle X-ray scattering or neutron scattering can be used to extract information on intra- and inter-micellar ordering [25]. Neutron scattering has the advantage compared to X-ray scattering that the contrast between different parts of the system (e.g. within the micelle or between the micelle and the solvent) can be varied by selective deuteration of solvent and/or one of the blocks. In dilute solution, only intramicellar structure contributes to the scattered intensity (the so-called form factor) and this can be modelled to provide information on micelle size and shape. The simplest model is that of a uniform hard sphere, although more sophisticated models are usually required for high-quality data fitting [54]. The intermicellar structure factor dominates at higher concentrations. It can be analysed using the hard sphere model [54] to give information on the micellar radius, and the micellar volume fraction. Where attractive interactions

between micelles are significant, these also influence the structure factor and this can be modelled using the ‘‘sticky sphere’’ approximation [55].

A diverse range of theoretical approaches have been employed to analyse the structure of block copolymer micelles, and for micelle formation [25]. The first models were based on scaling relationships for polymer ‘‘brushes’’ and give predictions for the dependence of micelle dimensions on the size of the blocks, as well as the association number of the micelle. A ‘‘brush’’ theory by Leibler and coworkers [56] enables the calculation of the size and number of chains in a micelle and its free energy of formation. The fraction of copolymer chains aggregating into micelles can also be obtained. Self-consistent field theory was first applied to predict the cmc of a diblock in a homopolymer matrix, and then applied to block copolymers in solution. The lattice implementation of SCF theory has been applied by Linse and coworkers [57] to analyse the dimensions of micelles for specific (Pluronic) block copolymers.

In addition to applications as surfactants and in personal care products, block copolymer micelles have been extensively investigated as nanoparticles for solubilizing active agents for drug delivery [52], or as ‘‘nanoreactors’’ for the production of inorganic nanoparticles, e.g. of metals with potential applications in catalysis [58]. An alternative approach is to form vesicles (bilayers wrapped round into a spherical shell) [59]. These may be crosslinked or polymerized to form hollow-shell nanoparticles [60].

At higher concentrations, block copolymers in solution form a variety of lyotropic mesophases [25]. Due to fact that such phases possess a finite yield stress and so usually do not flow under their own weight, these are often termed gels. However, it must be emphasized that the gel properties result from the ordered microstructure rather than any crosslinks between polymer chains as in a conventional polymer gel. The symmetry of the ordered phase formed largely depends on the interfacial curvature, as for conventional amphiphiles, however, the phase behaviour can also be understood by mapping it onto that for block copolymer melts [50]. Shear can be used to orient block copolymer gels as for block copolymer melts. Large-amplitude oscillatory shear or high shear rate steady shear both lead to macroscopic orientation of the structures. In the case of cubic phases in particular the flow mechanisms are complex, as is the rheological behaviour with interesting nonlinear effects such as plateaus in the flow curve.

Theory for the phase behaviour of block copolymers in semidilute or concentrated solution is less advanced than that for melts or dilute solutions due to the complexity of interactions between polymer and solvent. The two main methods

developed have been (a) SCF theory for density profiles and domain spacing scalings and (b) weak-segregation limit calculations of the shift in the order–disorder transition temperature with changing concentration. SCF theory calculations by Linse and coworkers [61] have produced phase diagrams for specific Pluronic copolymers in aqueous solution that are in remarkably good agreement with those observed experimentally. Simulations using the dynamic density functional theory have also yielded surprisingly accurate predictions for the sequence of phases obtained on varying concetration [62].

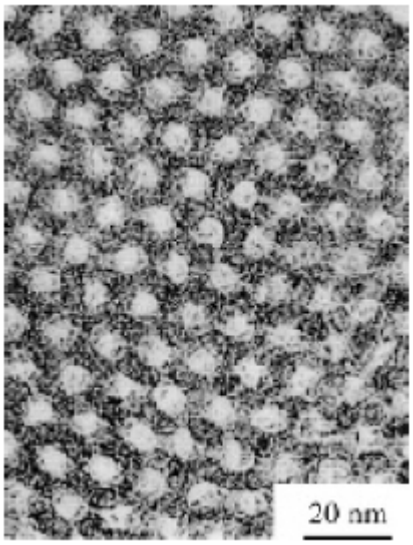

Figure 1.17 TEM image of calcined silica structure templated using an acidic solution of Pluronic poly(oxyethylene)-*b*-poly(oxypropylene)-*b*-poly(oxyethylene) triblock [63]

Lyotropic block copolymer mesophases can be used to template inorganic materials such as silica [64], this producing materials with a high internal surface area that could be useful in catalysis or separation technology. Figure 1.17 shows a transmission electron micrograph of hexagonal mesoporous silica, templated using a Pluronic block copolymer.

1.4 AZOBENZENE BASED POLYMERS: PROPERTIES AND USAGE

1.4.1 INTRODUCTION

Azobenzene, with two phenyl rings separated by an azo (–N=N–) bond, serves as the parent molecule for a broad class of aromatic azo compounds. These chromophores are versatile molecules and have received much attention in research areas both fundamental and applied. The strong electronic absorption maximum can be tailored by

ring substitution to fall anywhere from the ultraviolet to red-visible regions, allowing chemical fine-tuning of color. This, combined with the fact that these azo groups are relatively robust and chemically stable, has prompted extensive study of azobenzene-based structures as dyes and colorants[65]. The rigid mesogenic shape of the molecule is well suited to spontaneous organization into liquid-crystalline (LC) phases, and hence polymers doped or functionalized with azobenzene- based chromophores (azo polymers) are common as LC media [66]. With appropriate electron donor/acceptor ring substitution, the π electron delocalization of the extended aromatic structure can yield high optical nonlinearity, and azo chromophores have seen extensive study for nonlinear optical applications as well [67]. One of the most interesting properties of these chromophores, is the readily induced and reversible isomerization about the azo bond between the *trans* and the *cis* geometric isomers [68], and the geometric changes that result when azo chromophores are incorporated into biopolymers and other polyelectrolytes. This light-induced interconversion allows systems incorporating azobenzene to be used as photoswitches, effecting rapid and reversible control over a variety of chemical, mechanical, electronic, and optical properties.

1.4.2 PHOTOISOMERIZATION OF AZOBENZENE

Although not restricted to azobenzene groups alone, photoisomerization is a property of molecules in which energy (light) results in the population of stable and isolable photostationary states, which confers the molecule a particularly stable configuration, or molecular structure [69]. In the case of photoinduced cis-trans isomerization in azobenzene groups, this involves the breaking of single bonds (vs. conformational change in conformers) wherein the orientation of the priority R group (cis and trans isomer) defines the configuration (Fig. 2.11). This configurational change defines the shape and orientation of the molecule. The photoisomerization of azobenzene groups is perhaps the most well known photochemical isomerization phenomena [70]. There is a vast amount of literature on photoisomerization of azobenzene and its derivatives in solution, bulk, doped and functionalized glassy polymers, and thin films [71].

The basic requirement of a successful molecular switch is the presence of two distinct forms of the molecule that can be interconverted reversibly by means of an external stimulus, such as light, heat, pressure, magnetic or electric fields, pH change, or chemical reaction. Irradiation of azobenzene-containing materials induces reversible

isomerization between the two isomers making azobenzene light-switchable molecules (photoswitches). As described earlier, the photoisomerization of azobenzene is accompanied by significant changes in the absorption spectra, structure, and dipole moment of the molecule. These changes can thus alter properties of the surrounding environment by switching them "on" or "off". The following sections review physical properties that can be modulated by light, with emphasis on structural changes, surface properties, binding affinity, catalytic activity, conductivity, permeability, complexation behavior, and stereochemistry.

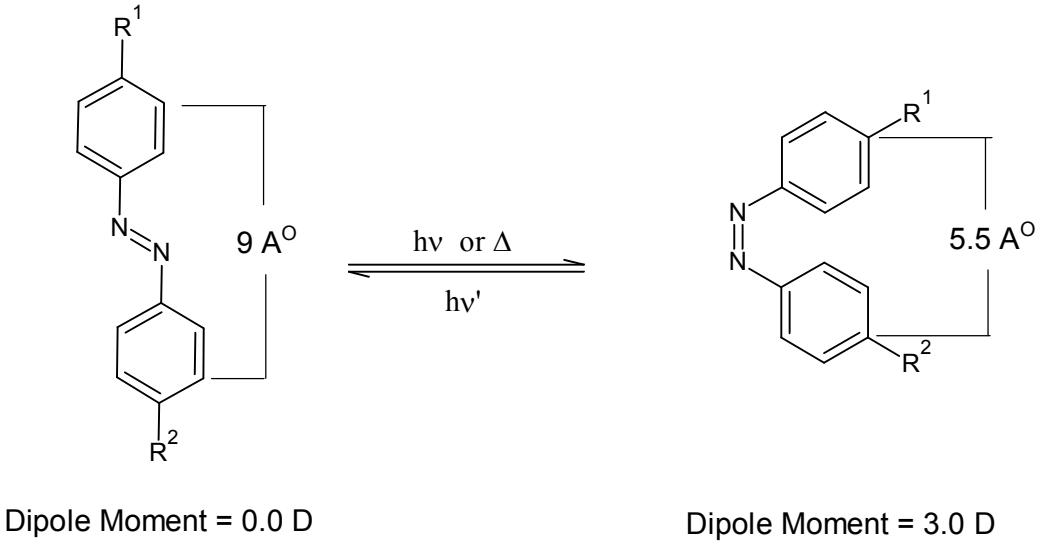

Figure 1.18 Photoisomerization of the azobenzene molecule showing change in size and dipole moment with irradiation.

1.4.3 AZOBENZENE CHROMOPHORES

For the purposes of classification of geometrical photoswitching, the nature and behavior of an azobenzene based chromophore can be described well by three variables: (1) the electronic absorbance maximum λ_{max}; (2) the dipole moment μ; and (3) the shape, which can be roughly quantified by the aspect ratio r_a and the effective occupied volume, OV. Each of these variables can be controlled synthetically with the introduction of appropriate ring substituents, or in the case of r_a also by linking together additional phenyl rings with azo bonds to form dis- and tris-azobenzene dyes [72]. For the wide range of λ_{max} values displayed by various azo chromophores (and hence the wide range of colors and properties) a useful classification scheme was introduced by

Rau. Azo aromatic chromophores can be considered to belong to one of three spectral types based on the energetic ordering of their (π*, *n*) and (π*, π) electronic states as that of azobenzene type, aminoazobenzene type, or pseudo-stilbene type [73]. Azobenzene-type molecules (shown in Fig. 2.12), display a low-intensity π* ← *n* absorption band in the visible region and a high-intensity π* ← π band in the UV. *Ortho*- or *para*-substitution with an electron-donating group (such as an $–NH_2$ amino) leads to the aminoazobenzene type where the π* ←*n* and π* ← π bands are very close or overlapped in the violet or near-visible UV, due to an increase in the π orbital energy and a decrease in the energy of the π* orbital. This effect is enhanced with the 4 and 4′ position substitution of electron donor and electron acceptor (push/pull) substituents (such as an amino and $–NO_2$ nitro group, respectively), which shifts the π* ← π transition band toward the red (past that of the π* ← *n*) to assume a reverse order, and places the molecule in the pseudo-stilbene spectral class. The three classes then exhibit colors of yellow, orange, and red, respectively, they will isomerize with characteristic rates and to characteristic extents, and hence in general they will interact differently with light of a given wavelength when incorporated into polymers

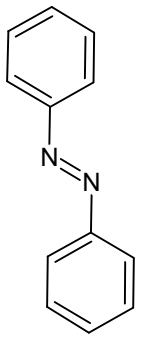

Figure 1.19 The structure of azobenzene.

Substitution with electron donor and/or electron acceptor groups increases the electric dipole moment (μ) of the chromophore as well [74]. Azo chromophores both respond to an external electric field and generate one, which contributes to the local EM environment, and can influence neighboring dipoles as well. The result of this is a tendency toward directional alignment of the chromophores with an applied external field (poling), which is used extensively in nonlinear optical (NLO) studies and applications. The rates and extent of this alignment (if it can be induced at all) depend strongly on the local viscosity of the matrix. In general, one needs to bring a system to

the rubbery or melt phase for an appreciable response. The geometrical shape descriptions of azo chromophores are less easily quantified, but in general can be described by the aspect ratio and the occupied volume.

1.4.4 CONSEQUENCES OF ISOMERIZATION

Photoinduced isomerization of azo aromatics proceeds with a structural change as it reflected in the change in geometry and polarity of the chromophore. The conversion from *trans* to *cis* azobenzene involves a decrease in the distance between the 4 and 4' ring positions from about 9.0 A to 5.5 A. The *trans* azobenzene isomer has no dipole moment whereas the dipole moment of the nonpolar *cis* compound is 3.0 D. This change in the dipole moment between the two isomers is large enough to influence the helical and random coil structures in some azo modified polypeptides. In such cases, the photoisomerization of the azo units produces a variation in the local charge density of the environment around the helical backbone, thus causing a conformational change. The two isomers of azo aromatics exhibit different absorbance spectra, different free volume requirements, and different electrochemical properties. These properties when manifested in polymers are useful probes of conformational dynamics and estimation the free volume of macromolecules, as well as in designing photoresponsive polymers.

While some research has focused solely on the kinetics of azo aromatics, the majority of the interest is realized in both the direct and indirect consequences of isomerization. It is well known that *trans-cis* reactions are accompanied by significant changes of polymer properties, such as the phase, conformation and optical properties. During the isomerization, there are large structural changes in both geometry and dipole state of the chromophore, making the azobenzene unit potentially useful for photocontrol of polymer structure. For instance, isomerization in liquid crystals is known to destroy or rearrange any ordered systems. This results from the large geometrical change that occurs upon isomerization. Of importance to this work, the rates of isomerization in solution have also been shown to be sensitive to the local environment surrounding the azobenzene molecule, such as the polarity and pH of the solvent, as well as ion and polymer concentration. These high sensitivities have thus facilitated the use of azobenzene molecules as excellent probes of the local polymer environment.

1.5 STIMULI RESPONSIVE AZOBENZENE BLOCK COPOLYMER FOR DRUG DELIVERY

Block copolymers (BCPs) can self-organize into micelles in solution if the solvent is good for one block but bad for the other, i.e., being block selective. In the case of amphiphilic BCPs, their micelles in aqueous solution have a compact core region formed by the hydrophobic block and a shell (corona) formed by the hydrophilic block that ensures their solubility (or dispersion) in water. Like micelles of small-molecule surfactants, the decisive parameter controlling the non-covalent micellar association of BCPs is the hydrophilic/hydrophobic balance that is governed by variables such as the relative lengths of the two blocks and their interactions with water determined by their chemical structures. Studies in recent years have established a general design principle for light-dissociable BCP micelles, which is schematically illustrated in Figure 1.20.

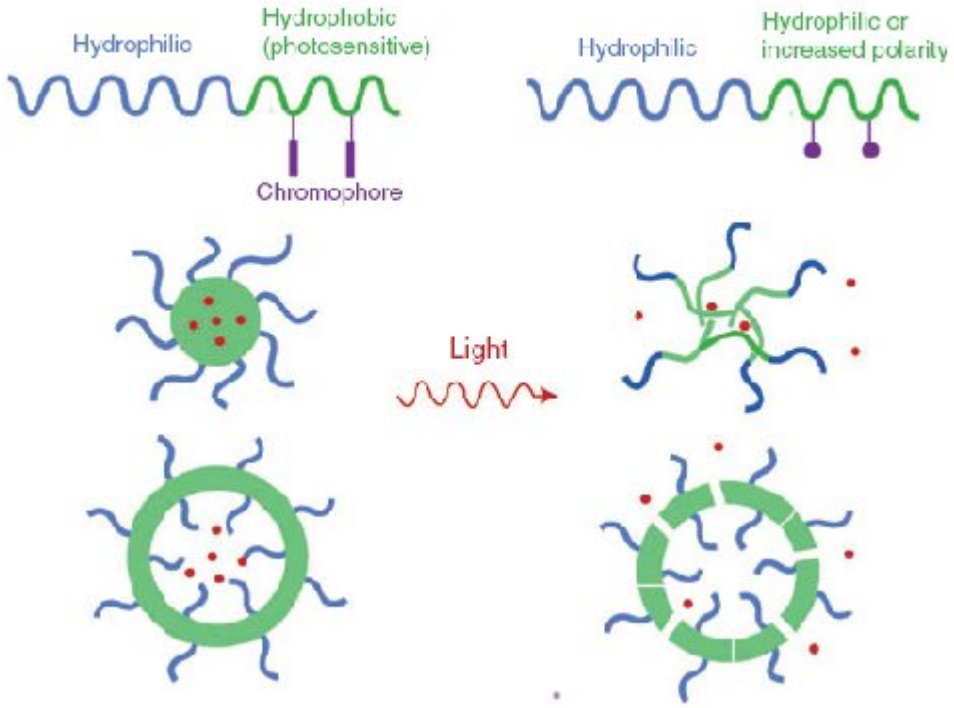

Figure 1.20 Schematic illustration of the rational design of light-dissociable block copolymer core-shell micelles or vesicles. The photoreaction of the chromophore on the hydrophobic polymer either increases its polarity or converts it into a hydrophilic polymer; in both cases, the hydrophilic/hydrophobic balance can be shifted toward the destabilization of the micellar association.

The hydrophobic block of the amphiphilic BCP is designed to be a lightresponsive polymer having a chromophore in its structure as pendent groups. The BCP can form core-shell micelles or vesicles for encapsulation of hydrophobic and hydrophilic agents, respectively (polymer vesicles can also load hydrophobic agents in the membrane, which is not depicted in Fig. 1.20). Upon illumination, the photoreaction of the chromophore shifts the hydrophilic/hydrophobic balance toward the dissociation of the micellar aggregates. Two types of photoreactions can lead to this result. In one, the photoreaction of the chromophore increases significantly the polarity of the hydrophobic polymer so that it is no longer hydrophobic enough to hold the micellar association. In the other case, the photoreaction of the dye causes such a structural change that the hydrophobic polymer is simply converted into a hydrophilic one. In the latter case, the basic condition for BCP micelle formation is gone, and their micelles should be dissociated by light.

On the basis of this rational design scheme, a few light-switchable micelles and vesicles have been obtained. Zhao and coworkers have synthesized Azobenzence based BCPs. The hydrophilic block was a random copolymer of Poly(*tert*-butylacrylate-co-acrylic acid) [P(*t*BA-*co*-AA)], the hydrophobic block (PAzoMA) is a side-chain liquid crystalline polymethacrylate bearing the azobenzene chromophore that can undergo the reversible trans-cis photoisomerization upon UV and visible light irradiation. This diblock copolymer, P(*t*BA-*co*-AA)-*b*-PAzoMA, was prepared by synthesizing first P*t*BA-*b*-PAzoMA using atom transfer radical polymerization (ATRP) and then by partially hydrolyzing the *t*BA units. Polymer coreshell micelles and vesicles were obtained, and they displayed light-controllable reversible dissociation and formation [75].

1.6 REFFERENCES

1. M. Szwarc, M. Levy, R. Milkovish, J. Am. Chem. Soc. 78, 2656, 1956
2. R. Quirik, Anionic polymerization. In Encyclopedia of Polymer Science and Technology; John Wiley and Sons: New York, 2003.
3. M. Pitsikalis, S. Pispas, J. W. Mays, and N. Hadjichristidis, Adv. Polym. Sci. 135, 1 (1998).
4. N. Hadjichristidis, N. Pispas, M. Pitsikalis, H. Iatrou, and C. Vlahos, Adv. Polym.Sci. 142, 71 (1999).
5. Z.-G. Yan, Z. Yang, C. Price, and C. Booth, Makromol. Chem., Rapid Commun. 14,725 (1993).
6. K. Hong, D. Uhrig, J. Mays, Living polymerization, Curr Opin Solid state Mater Sci. 531,4 (1999)
7. K. Matyjaszewski ‘‘Controlled Radical Polymerization’’ in ACS Symp. Ser. 685, K. Matyjaszewski Ed., American Chemical Society, Washington DC, Chapter 1 (1998)
8. Benoit D., Chaplinski V., Braslau R., Hawker C. J., J. Am. Chem. Soc, 121: 3904(1999) Benoit D., Grimaldi S., Robins S., Finet J. P., Tordo P., Gnanou Y., J. Am. Chem. Soc, 122: 5929 (2000) Chong Y. K., Ercole F., Moad G., Rizzardo E., Thang S. H., Anderson A. G., Macromolecules, 32: 6895 (1999)
9. Wang, J.; Matyjaszewski, K. J. Am. Chem. Soc. 1995, 117, 5614-5615
10. Matyjaszewski K., Patten T. E., Xia J., J. Am. Chem. Soc, 119: 674 (1997)
11. Beers K. L., Boo S., Gaynor S. G., Matyjaszewski K., Macromolecules, 32: 5772 (1999)
12. Davis, K. A.; Matyjaszewski, K. Macromolecules, 33,4093 (2000)
13. J. Chiefari, Y. K. Chong, F. Ercole, J. Krstina, J. Jeffery, T. P. T. Le, R. T. A. Mayadunne, G. F. Meijs, C. L. Moad, G. Moad, E. Rizzardo, S. H. Thang, Macromolecules 1998, 31(16), 5559–5562
14. Watanabe, H. (1998) In Structure and Properties of Multi-Phase Polymeric Materials, Araki, T., Tran-Cong, Q. and Shibayama, M., Eds., Marcel Dekker, New York, 317–360. Vigild, M. E., Chu, C., Sugiyama, M., Chaffin, K. A. and Bates, F. S. (2001) Macromolecules 34: 951–964.Hermel, T. J., Wu, L., Hahn, S. F., Lodge, T. P. and Bates, F. S. (2002) Macromolecules 35: 4685–4689

15. C. S. Patrickios, C. Forder, S. P. Armes, N. C. Billingham, J. Polym. Sci. Polym. Chem., 35, 1181– 1195 (1997).
16. K. L. Hong, Y. N. Wan, J. W. Mays, Macromolecules, 34, 2482–2487 (2001).
17. K. Jankova, X. Chen, J. Kops, W. Batsberg, Macromolecules, 31, 538 (1998)
18. K. Beers, S. Boo, S. G. Gaynor, K. Matyjaszewski, Macromolecules, 32, 5772 (1999)
19. Krzysztof Matyjaszewski, Simion Coca, Scott G. Gaynor, Mingli Wei, and Brian E. Woodworth, Macromolecules, 30, 7348 (1997)
20. S. Grimaldi, J. Finet, A. Zeghdaoui, P. Tordo, D. Benoit, Y. Gnanou, M. Fontanille, P. Nicol, J.P. Pierson, Am. Chem. Soc. Div. Polym. Chem., 38, 651 (1997)
21. E. Yoshida and A. Sugita. Macromolecules 29 (1996), p. 6422
22. S. Coca, H. Paik, K. Matyjaszewski, Macromolecules, 30, 6513 (1997)
23. D. Arriola,, Carnahan, E., Hustad, P., Kuhlman, R., Wenzel, T. "Catalytic Production of Olefin Block Copolymers via Chain Shuttling Polymerization" Science Vol. 312 May 2006
24. F. S. Bates,; Fredrickson, G. H. Annu. Rev. Phys. Chem., 41, 525-557. **(**1990)
25. I. W. Hamley, The Physics of Block Copolymers (Oxford University Press, Oxford, 1998]
26. D. A. Hajduk, P. E. Harper, S. M. Gruner, C. C. Honeker, G. Kim, E. L. Thomas, and L. J. Fetters, Macromolecules 27, 4063 (1994)
27. C. D. Han, D. M. Baek, J. K. Kim, T. Ogawa, N. Sakamoto, and T. Hashimoto, Macromolecules 28, 5043 (1995).
28. S. M. Mai, J. P. A. Fairclough, I. W. Hamley, R. C. Denny, B. Liao, C. Booth, and A. J. Ryan, Macromolecules 29, 6212 (1996).
29. V. P. Voronov, V. M. Buleiko, V. E. Podneks, I. W. Hamley, J. P. A. Fairclough, A. J. Ryan, S.-M. Mai, B.-X. Liao, and C. Booth, Macromolecules 30, 6674 (1997).
30. F. S. Bates and G. H. Fredrickson, Macromolecules 27, 1065 (1994).
31. G. H. Fredrickson and E. Helfand, J. Chem. Phys. 87, 697 (1987).
32. E. Helfand and Z. R. Wasserman, in Developments in Block Copolymers 1, edited by I. Goodman (Applied Science, London, 1982), p. 99.
33. L. Leibler, Macromolecules 13, 1602 (1980).
34. M. W. Matsen and F. S. Bates, Macromolecules 29, 1091 (1996).

35. E. F. David and K. S. Schweizer, J. Chem. Phys. 100, 7784 (1994).
36. V. Ganesan and G. H. Fredrickson, Europhys. Lett. 55, 814 (2001).
37. M. J. Folkes and A. Keller, in The Physics of Glassy Polymers, edited by R. N. Haward (Applied Science, London, 1973), p. 548.
38. K. Almdal, K. Mortensen, K. A. Koppi, M. Tirrell, and F. S. Bates, J. Phys. France II 6, 617 (1996).
39. M. W. Matsen, J. Chem. Phys. 106, 7781 (1997).
40. K. Liu, S. M. Baker, M. Tuominen, T. P. Russell, and I. K. Schuller, Phys. Rev. B 63, 060403(R) (2001).
41. M. Park, C. Harrison, P. M. Chaikin, R. A. Register, and D. H. Adamson, Science 276, 1401 (1997).
42. G. Widawski, M. Rawiso, and B. Franc¸ois, Nature 369, 387 (1994).
43. D. Ausserre´,D. Chatenay, G. Coulon, and R. Collin, J. Phys. France 51, 2571 (1990).
44. S. H. Anastasiadis, T. P. Russell, S. K. Satija, and C. F. Majkrzak, Phys. Rev. Lett. 62, 1852 (1989).
45. N. Rehse, A. Knoll, M. Konrad, R. Magerle, and G. Krausch, Phys. Rev. Lett. 87, 035505 (2001).
46. S. Collins, T. Mykhaylyk, and I. W. Hamley, unpublished work (2002).
47. D. G. Walton, D. J. Kellogg, A. M. Mayes, P. Lambooy, and T. P. Russell, Macromolecules 27, 6225 (1994).
48. G. H. Fredrickson, Macromolecules 20, 2535 (1987).
49. M. S. Turner, M. Rubinstein, and C. M. Marques, Macromolecules 27, 4986 (1994).
50. K. J. Hanley, T. P. Lodge, and C.-I. Huang, Macromolecules 33, 5918 (2000).
51. G. Wanka et al. Macromolecules 27, 4145 (1994).
52. I. R. Schmolka, in Polymers for Controlled Drug Delivery, edited by P. J. Tarcha (CRC Press, Boston, 1991).
53. C. Booth and D. Attwood, Macromol. Rapid Comm. 21, 501 (2000).
54. J. S. Pedersen, Adv. Colloid Interface Sci. 70, 171 (1997).
55. Y. Liu, S.-H. Chen, and J. S. Huang, Macromolecules 31, 2236 (1998).
56. L. Leibler, H. Orland, and J. C. Wheeler, J. Chem. Phys. 79, 3550 (1983).
57. P. Linse, Macromolecules 26, 4437 (1993).

58. M. V. Seregina, L. M. Bronstein, O. A. Platonova, D. M. Chernyshov, P. M. Valetsky, J. Hartmann, E. Wenz, and M. Antonietti, Chem. Mater. 9, 923 (1997).
59. L. Luo and A. Eisenberg, J. Am. Chem. Soc. 123, 1012 (2001).
60. C. Nardin, T. Hirt, J. Leukel, and W. Meier, Langmuir 16, 1035 (2000).
61. M. Svensson, P. Alexandridis, and P. Linse, Macromolecules 32, 637 (1999).
62. B. A. C. van Vlimmeren, N. M. Maurits, A. V. Zvelinodvsky, G. J. A. Sevink, and J. G. E. M. Fraaije, Macromolecules 32, 646 (1999).
63. D. Zhao et al. Science 279, 548 (1998)
64. P. Kipkemboi, A. Fogden, V. Alfredsson, and K. Flodstro¨m, Langmuir 17, 5394 (2001).
65. K. Ichimura, H. Durr, H. Bouas. –Laurent. Eds., Elsevier. Amsterdam. P. 903. 1990
66. H. Zollinger. Colour Chemistry., VCH, Weinheim, 1987.
67. S. Kwolek, P. Morgan, J. Schaefgen, John Wiley, New York, Vol 9, p. 1. 1985.
68. L. R. Dalton, A. W. Harper, R. Ghosn, W. H. Steier, M. Ziari, H. Fetterman, Y. Shi, R. V. Mustacich, A. Jen, K. Y. Shea, Chem. Mater. 7, 1060, 1995.
69. H. Rau, J. Rabek, Ed. CRC Press, Boca Raton, FL, Vol II, Chap. 4. 1990
70. L. Ichimura, Chem, Fev. 100, 1847, 2000
71. T. Radeva edited by M. Dekker, Inc., Surfactant Scinece Series, Vol. 99, 2001
72. Y. Dirix, T. Tervoort, C. Bastiaansen, Macromolecules, 30, 2175, 1997.
73. D. I. Gittins, F. J. Caruso, Phys. Chem. B, 105, 6846, 2001
74. M. A. Omar, Chap. 8, Addison Wesley, London, 1974.
75. G. Wang, T. Xia, Y. Zhao, Macromolecules, 37, 8911, 2004

CHAPTER 2: EXPERIMENTAL WORK

2.1 SYNTHESIS

2.1.1 SYNTHESIS OF ACROLOYL CHLORIDE

Materials

Acrylic acid (Merk), benzoyl chloride (Riedel), and hydroquinone (Rieel) were used as received.

Procedure

Acryloyl chloride was prepared in lab in accordance to the Figure 2.1 given below. In general, 43.2gm (0.6moles) of acrylic acid, 168.8gm (1.2moles) of benzoyl chloride and 0.1gm hydroquinone were taken in a round bottom flask. The flask was then attached to an efficient distilling column to allow distillation at a reasonable rate. The glass ware assembly used for the synthesis of acryloyl chloride is shown in Figure 2.2 (The reaction was performed in a fume hood to avoid fumes of acryloyl chloride). The mixture was heated until it started to boil, and the resultant distillate was collected in a receiver immersed in ice and contained 0.1gm of hydroquinone. This was accomplished when the temperature at the top of column remained between 60-70°C for most of the distillation. When the temperature had reached 85°C the distillation was discontinued, and about 40gm of the crude product obtained. The crude product was redistilled again at 72-74°C to yield about 35gm of the final product. It was observed that the temperature registered could be several degrees below the true boiling point, due to the fact that the acid chloride was partially carried over by the hydrogen chloride given off by the reaction mixture[1].

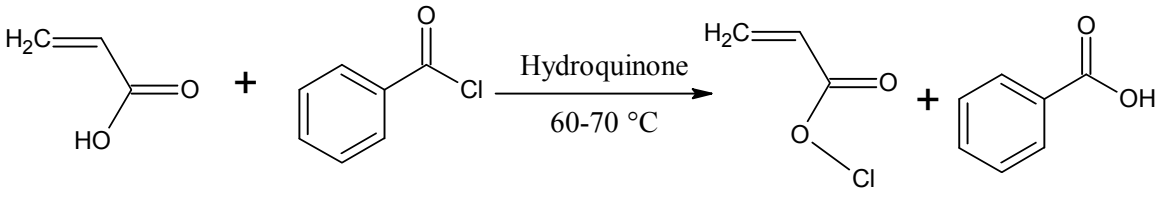

Acrylic acid Benzoyl chloride Acryloyl Chloride Benzoic Acid

Figure 2.1 Reaction of Acrylic acid and Benzoyl Chloride to form Acryloyl Chloride

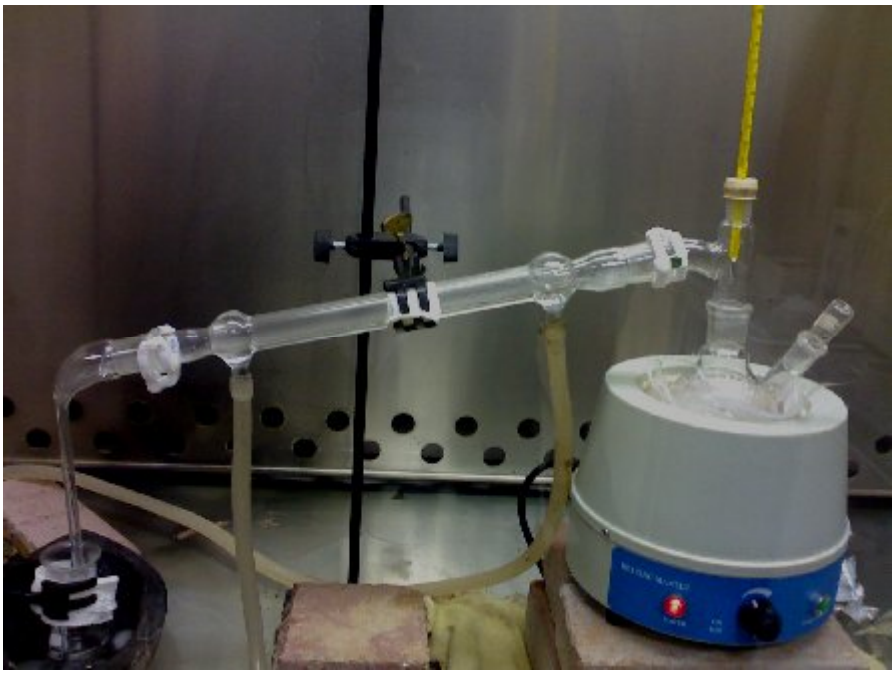

Figure 2.2 Glassware assembly used for the lab preparation of acryloyl chloride.

2.1.2 SYNTHESIS OF AZO-DYE

Materials

4-Nitroaniline (Fisher Scientific), phenol (Fisher Scientific), hydrochloric acid (Fisher Scientific), sodium nitrite (Merk), sodium hydroxide Merk) and sodium acetate (Fisher Scientific) were used as received.

2.1.2.1 PREPARATION OF DIAZONIUM SALT

In the current work, the diazonium salt of 4-nitroaniline was prepared. As described in the Figure 2.3. Typically, a mixture was prepared in a beaker by taking 0.05 mol of aniline derivative, 17mL (0.12mol) concentrated hydrochloric acid and 10 mL water. The prepared mixture was heated until it turned to a pellucid solution. This was followed by placing the mixture into an ice-salt bath and stirred rapidly with the aid of a magnetic stirrer while keeping the temperature about 0-5°C in order to precipitate the hydrochloride as fine crystals. To this cooled mixture, 20.4mL aqueous solution of sodium nitrite (3.507g, 0.05mol) was added drop wise with constant stirring, and the mixture was further stirred for one hour to obtain the diazonium salt solution. It is

important to mention that solution temperature should be kept less than 5°C to avoid decomposition reaction[2].

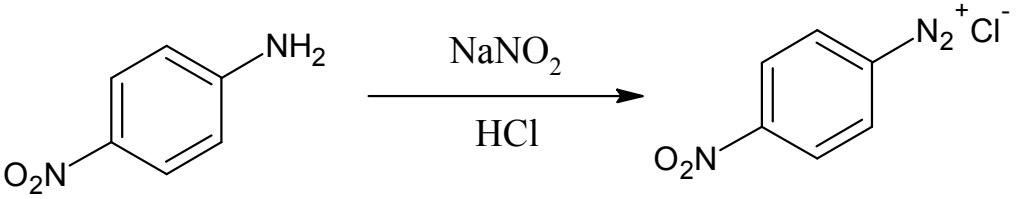

4-Nitroaniline Diazonium Salt

Figure 2.3 Formation of Diazonium Salt of 4-Nitroaniline

2.1.2.2 SYNTHESIS OF 4-[2-(4-NITROPHENYL)DIAZENYL] PHENOL DYE (NDP)

4-[2-(4-nitrophenyl)diazenyl]phenol dye (NDP) was prepared by carrying out the reaction between the diazonium salt of 4-nitroaniline and phenol as described by the Figure 2.4. For this reaction, a 10% solution of NaOH (4g, 0.05mol) was prepared in a small beaker, and phenol (4.71g, 0.05mol) was dissolved in it, while the whole mixture was cooled to lower than 5-10°C in an ice bath. If required, few grams of ice were added to keep the required low temperature. To the prepared cooled solution mixture, the cooled solution of the diazonium salt was slowly added drop wise while maintained the temperature below 5°C. The resultant mixture was vigorously stirred for further one hour, and then the saturated solution of sodium acetate was added to adjust pH value at 6-7. The temperature was kept at 0-10°C for further 3 hours, the obtained mixture was filtered by suction filtration and washed with a large excess of water. The product was dried under vacuum at room temperature to give 56% yield[2].

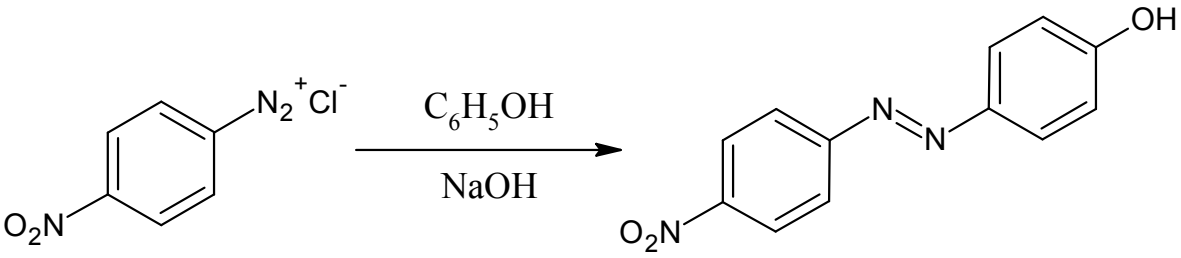

Diazonium Salt 4-[2-(4-nitrophenyl)diazenyl]phenol Dye (NDP)

Figure 2.4 Formation of NDP dye from Diazonium Salt

2.1.3 SYNTHESIS OF AZO-FUNCTIONALIZED MONOMER.

Materials

Analytical grade commercially available triethylamine (Fisher Scientific), chloroform (Fisher Scientific), hydrochloric acid (Fisher Scientific), and sodium hydroxide (Merk) were used as received. Acryloyl chloride was synthesized in the lab (see above) by reacting acrylic acid with benzoyl chloride (Riedel).

Procedure

2-propenoic acid,4-[2-(4-nitrophenyl)diazenyl]phenyl ester (NDP monomer) was prepared by reacting acryloyl chloride with azophenol dye in accordance to the Schotten-Bauman reaction. Figure 2.5 describes the synthesis of the monomer. In general, azophenol NDP dye (0.03mol), THF (120mL) and triethylamine (6mL) was added to a 250mL round bottom flask and the mixture was cooled with an ice bath. Acryloyl chloride (3.6g, 0.0396mol) diluted in THF (30mL) was added slowly and drop wise to the cool solution. The resultant mixture was vigorously stirred in an ice bath for one hour and then at room temperature for further 4 hours. [2]

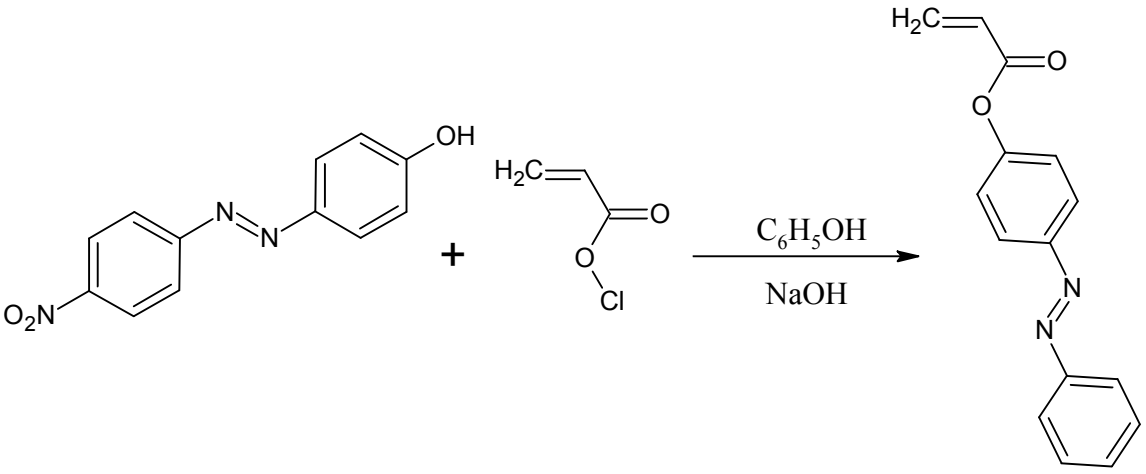

Dye NDP Acryloyl Chloride 4-[2-(4-nitrophenyl)diazenyl]phenyl ester(NDP Monomer)

Figure 2.5 Reaction of NDP Dye with Acryloyl Chloride to give NDP Monomer

Purification of NDP monomer

Chloroform (120mL) was added to the above mixture and then the mixture was washed by solution of HCl (300mL,pH=1) and 300mL of 3% NaOH in a 500mL

separating funnel. The chloroform phase was washed to neutrality with water and removed out to a distilling flask. After distillation, the crude product was purified by recrystallization from chloroform to give needle-like crystals of NDP azo monomer. Yield was about 50% (0.012mol). Both the NMR and IR spectrums of the prepared monomer confirmed the presence of vinyl bond (CH_2=CH) in the monomer structure[2].

2.1.4 ATOM TRANSFER RADICAL POLYMERIZATION

2.1.4.1 SYNTHESIS OF POLY-TERT-BUTYL ACRYLATE MACROINITIATORS

Materials

t-butylacrylate, Copper(I) Bromide, Copper(II) Bromide. PMDETA, Ethyl-2-bromopropionate were used as received. THF was used after drying over sodium wire.

Procedure

CuBr and $CuBr_2$ were added to a dry round bottom flask (rbf). The flask was sealed with a rubber septum, degassed and back-filled with nitrogen three times, and left under nitrogen. Dried THF, PMDETA and t-BA was added using syringes purged with nitrogen (details of feed ratios is presented in Table 3.1), and the solution was stirred until the Cu complex had formed. This can be clearly visualized through a change of the solution from cloudy and colorless to clear and light green. After complex formation ethyl 2-bromoporpionate was added to the flask and the mixture was freezed by immersing flask in liquid nitrogen and then evacuated any gas present in the flask, then the mixture was allowed to melt. This was repeated to more times to ensure that no other gas remains in flask and only vapours of THF fill the empty space to flask. Then flask was placed on hot plate thermostated at 60°C. After about 8 hours the rubber septum was removed and the mixture was diluted with Dry THF. [3]

2.1.4.2 SYNTHESIS OF POLY(TERT-BUTYLACRYLATE)-BLOCK-POLY(NDP) POLYMERS, P(t-BA-*b*-NDP)

The solution of prepared macroinitiator was used for the synthesis of block copolymer. 1mL of macroinitiator solution was taken in a dry round bottom flask and

excess amount of NDP monomer (0.5gm) is also added to this mixture. Sufficient amount of dry THF also added so that the NDP monomer is completely dissolved. The flask is then sealed with rubber septum, the mixture was freezed by immersing flask in liquid nitrogen and then evacuated any gas present in the flask, and then the mixture was allowed to melt. This was repeated three more times to ensure the removal of any air present in flask. The flask was then placed on hot plate thermostated at 60°C. After about 24 hours the rubber septum was removed and the mixture was diluted with Dry THF.

2.2 CHARACTERIZATION OF MATERIALS

Various characterization techniques were used to determine the structure and molecular weights of the developed materials.

2.2.1 UV-VISIBLE AND INFRARED SPECTROSCOPIES

The UV-Visible absorption spectrums of the prepared azobenzene dye and monomer were measuered in THF solvent. A Perkin-Elmer Lambda 20 spectrophotometer was used for this purpose, and shown in Figure 2.6. The IR spectra were recorded using the facility at SCME.

Figure 2.6 Perkin Elmer Lambda 20 spectrophotometer, used to UV-Vis Spectra

A Perkin-Elmer Infra-red Spectrum 100 spectrometer (Fig. 2.7) was used to record IR spectra of the NDP Dye and NDP monomer. The samples were prepared in KBr pellets.

Figure 2.7 Perkin-Elmer FTIR Spectrum 100 spectrophotometer, used to obtain IR spectra.

Figure 2.8 Bruker 300 MHz spectrometer, used to obtain NMR spectra.

2.2.2 MONOMER AND POLYMER CHARACTERIZATION BY NMR SPECTROSCOPY

A Bruker 300 MHz NMR spectrometer as shown in Figure 2.8 was used to obtain NMR spectra and to determine the structure of the materials. Samples were prepared in d-DMSO or d-$CDCl_3$, and chemical shifts were referenced to the solvent peak at 2.49 and 7.25 ppm for ^1H spectra.

2.2.3 GEL PERMEATION CHROMATOGRAPHY (GPC)

Molecular weight and molecular weight distribution (MWD) of the prepared polymers were determined by using gel permeation chromatography (GPC). A Viscotek GPCmax VE-2001 with Model 302-050 Triple Detector Array with UV consisting of UV, RI Viscometer and RALS/LALS detectors in a controlled temperature oven was used to determine absolute molecular weights. THF was used as an eluent with a flow rate of 1 ml/min at a temperature of 35°C. A single point calibration of narrow molecular weight polystyrene standards was used. The GPC column was also equipped with column suitable for broad molecular weight measurement. The sample with accurate concentrations of 10-15 mg/mL in THF was injected for the determination of molecular weights. The GPC system used in the current work is shown in Figure 2.9.

Figure 2.9 Viscotek GPCmax VE-2001 with Model 302-050 Tripple Detector Array used for measurements of molecular weight.

2.3 REFFERENCES

1. G. M. Stampel, R. P. Cross, R. P. Mariella, J. Am. Chem. Soc, 72, 2299 (1950)
2. N. Li, J. Lu, Q. Xu, L. Wang, Optical Materials, 28, 1412 (2006)
3. K. A. Devis, K. Matyjaszewski, Macromolecules, 33, 4039 (2000)

CHAPTER 3: RESULTS AND DISCUSSION

3.1 CHARACTERIZATION OF PREPARED AZO-DYE AND AZO MONOMER

The prepared materials were characterized by IR spectroscopy and NMR spectroscopy to confirm their structures. The representative IR spectrums of the prepared NDP Dye and NDP monomer are shown in Figures 3.1 and 3.2. The IR frequencies values available in literature were used to identify the structures. For the prepared NDP azo dye, IR vibration values were found to be 3429 (ν_{OH}) and 1430 (δ_{OH}), around 1505 and 1339 ($\nu_{N\text{-}O}$ and $\nu_{C\text{-}N}$ of Ar-NO_2). Upon reaction with acryloyl chloride, the formation of ester bond was indicated by IR bands appearing at around 1730 and 1248 (νC=O and νC-O-C of ester), while peaks present in NDP dyes moves to around 1526 and 1343 ($\nu_{N–O}$ and $\nu_{C–N}$ of Ar–NO_2). Further, the preparation of monomer with vinylic bond indicated by the presence of 1610 cm^{-1} band (C=C stretching).

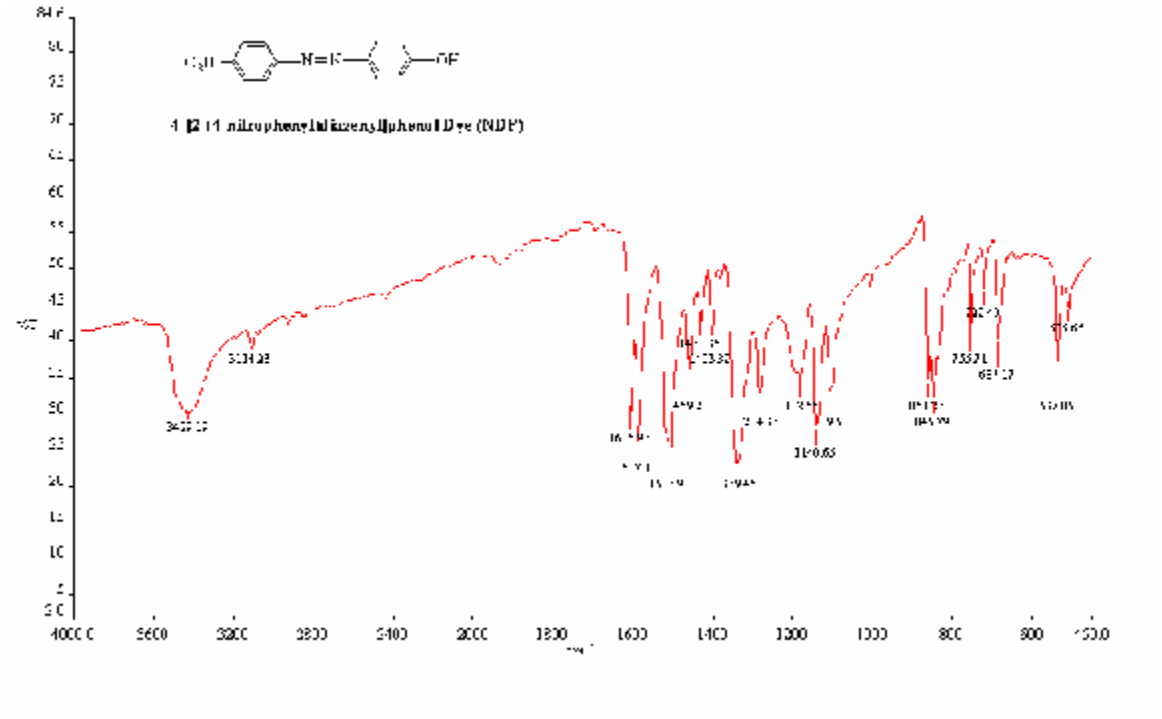

Figure 3.1: IR spectra of the synthesized NDP dye.

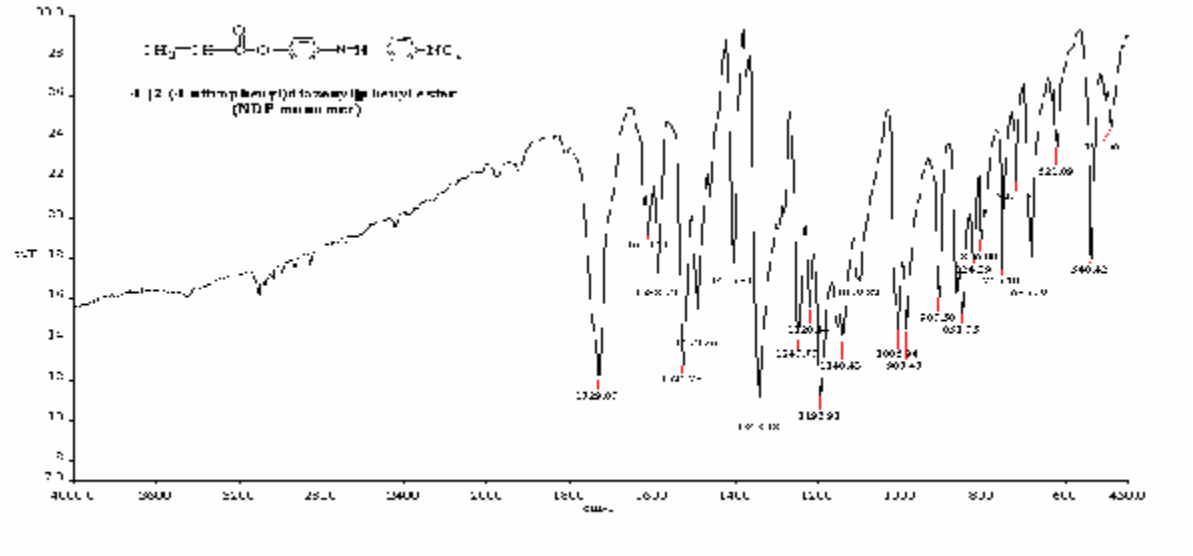

Figure 3.2: IR spectra of the synthesized NDP monomer.

The UV-Visible absorption spectra of NDP Dye and NDP azo monomer, in THF were found to be slightly changed as shown in Figures 3.3 and 3.4. The absorbance maximum of NDP dye is at 379 nm but as it is reacted with acryloyl chloride to produce NDP monomer with the introduction of conjugation in the form of double bond and a carbonyl group in it. The λ_{max} shows a blue shift as compared to NDP dye due to conjugation and absorbance maximum is obtained at 338nm as shown in Figure 3.4

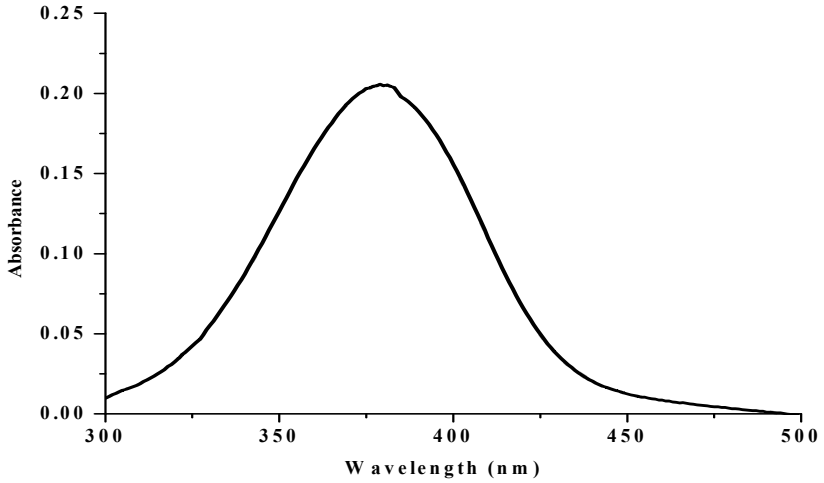

Figure 3.3 UV-Vis spectrum of NDP dye in THF solution.

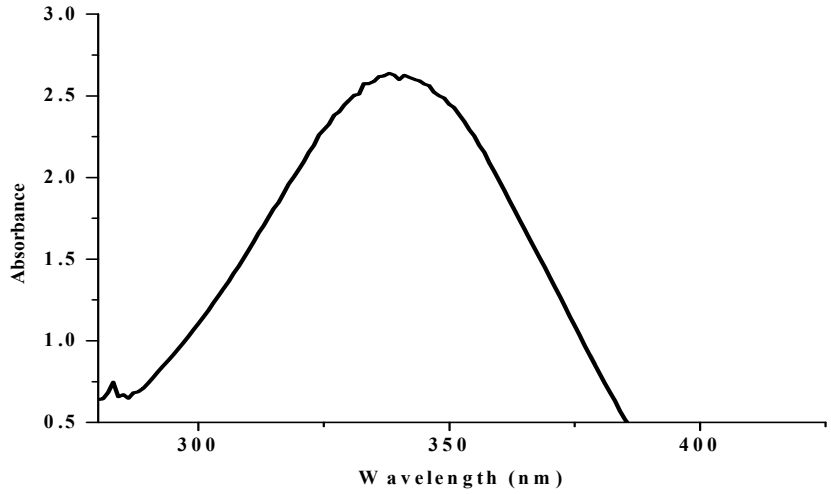

Figure 3.4 UV-Vis spectrum of NDP monomer in THF solution.

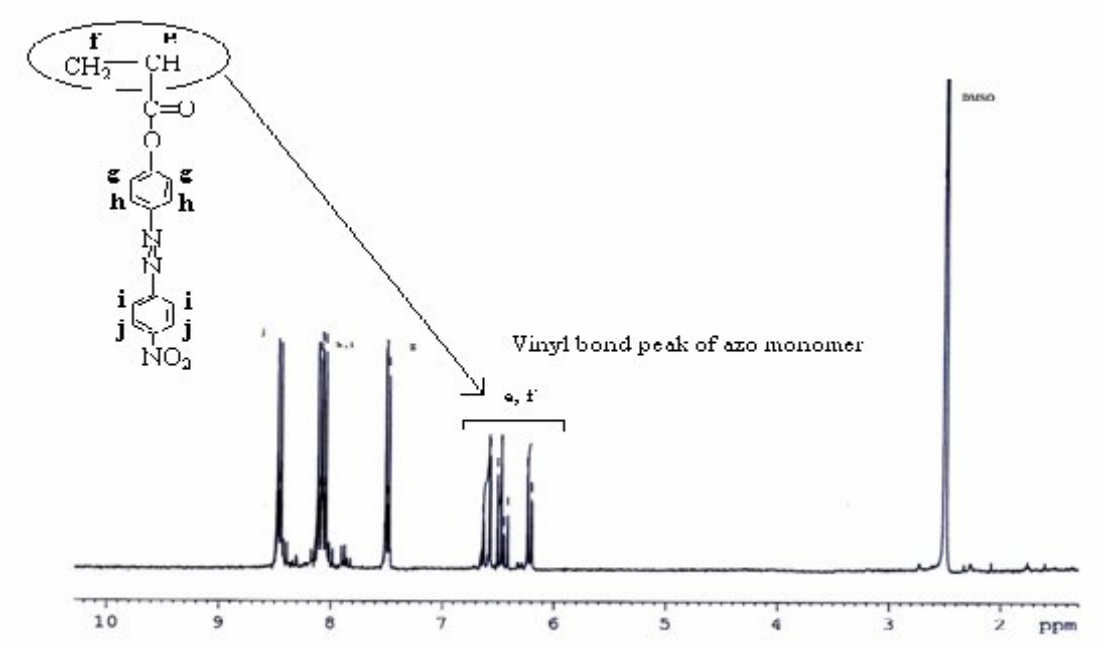

Figure 3.5 The ^{1}H NMR spectrum of the synthesized NDP monomer. Note the appearance of vinylic proton peaks in the structure of the monomer.

The prepared NDP monomer was also characterized by NMR spectroscopy, and the ^{1}H NMR spectrum of the prepared monomer is presented in Figure 3.5. The following chemical shifts confirmed the structure of NDP monomer δ(ppm) = 8.38 (2H, benzene ring protons), 8.08–7.90 (4H, benzene ring protons), 7.29 (2H, benzene ring protons),

6.83 and 6.38 (2H, protons of CH2=), 6.10 (1H, proton of –CH=). The appearance of vinylic protons peak at 6.10, 6.38 and 6.83 thus confirmed the occurance of reaction between azo phenol dye of NDP and acryloyl chloride monomer to yield NDP monomer.

3.2 ATOM TRANSFER RADICAL POLYMERIZATION (ATRP) TO PREPARE BLOCK COPOLYMERS.

Radical polymerization of acrylate monomers are characterized by propagating radicals of low steric bulk and high reactivity. These factors can affect the addition of the propagating radicals (Pn*) in the process of both conventional and controlled living radical polymerization such as ATRP in which an alkyl halide uses an initiator and a metal Mtn/L or Cu(I)/L in its lower oxidation state with a complexing ligand. The process involves the successive transfer of the halide from the dormant polymer chains (Pn-X) to the ligand metal complex, thus establishing a dynamic equilibrium between active and dormant species. The reaction mechanism involving different species during the ATRP process is shown in Figure 3.6.

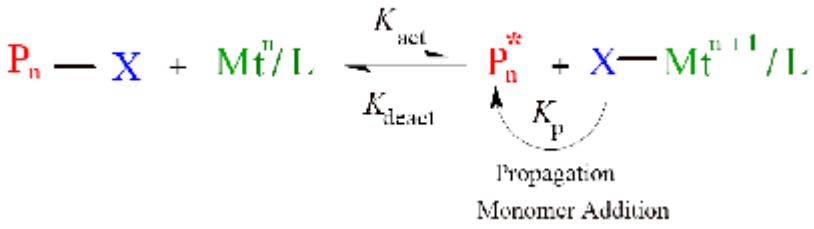

Figure 3.6 Reaction mechanism of ATRP involves dynamic equilibrium between active and dormant species.

Tertiary-butylacrylate (t-BA) has been polymerized using several different polymerization methods, including ionic, nitroxide-mediated, and metallocene-mediated reactions. However, t-BA polymerization by ATRP has several advantages such as good control of molecular weight because both initiation and deactivation are fast, allowing for all the chains to begin growing at approximately the same time while maintaining a low concentration of active species. Some early termination will lead to the formation of the Cu(II) species, but this is necessary to establish control via the persistent radical effect.

The acrylate monomers employed in the current ATRP polymerizations showed relatively good reactivity. The Reaction Scheme V and VI describe the synthesis of macroinitiator based on the blocks of t-BA monomer, and diblocks of NDP monomer, respectively. given in following Reaction Scheme V. The experimental conditions employed for polymerization are given in Table 3.1. The main characterization results of the ATRP polymerization are summarized in Table 3.2 and 3.3. Considering the experimental conditions employed for ATRP, a linear increase in molecular weight with conversion and narrow decreasing polydispersities are expected. Kinetics studies were not carried out in the current work, however, there is a decreases in MWD was observed as the block length increase in case of macroinitiator formation of P(t-BA) as shown in Figure 3.16. This observation indicates that the concentration of growing radicals is constant. Moreover, the experimental molecular weight agrees with the theoretical molecular weight estimated (see Figure 3.15).

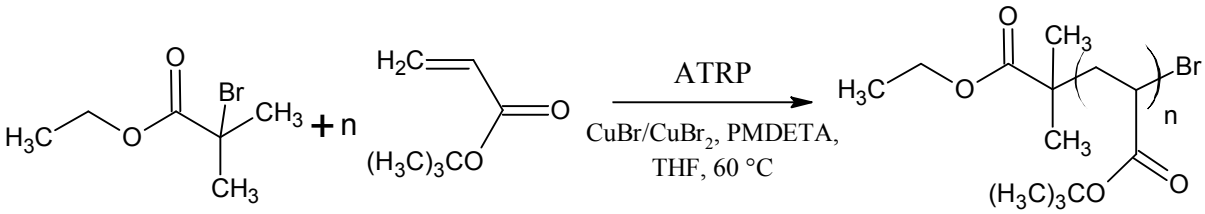

Ethyl 2-bromopropionate t-butylacrylate macroinitiator

Figure 3.7 Formation of Poly(tert-Butylacrylate) macroinitiator

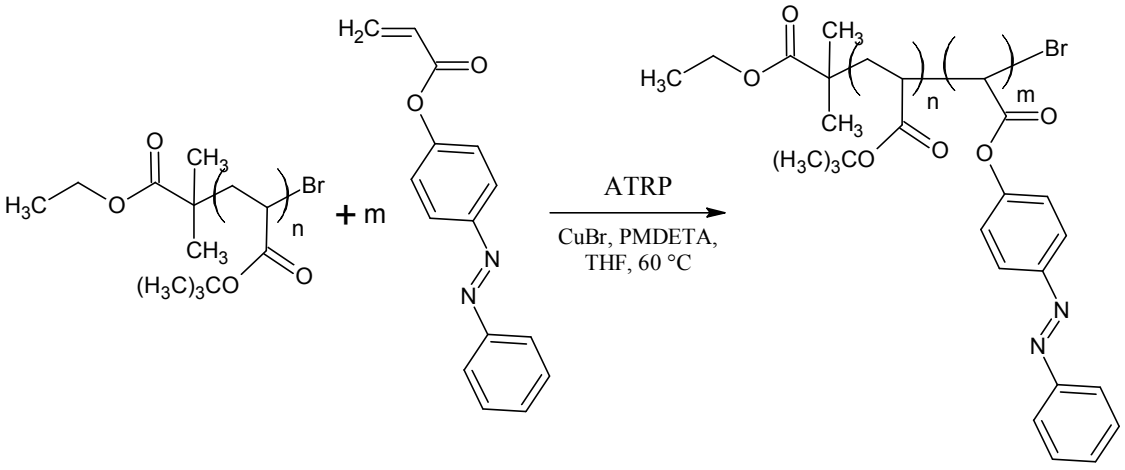

Macroinitiator NDP monomer P(tBA)-b-P(NDP)

Figure 3.8 Formation of P(t-BA)-b-P(NDP) block copolymer

The activation of the macroinitiators of P(t-BA) were evident from the extension of the polymer chain upon formation of the second block of the NDP monomer. The molecular weight of the second blocks of NDP monomer for all four blocks copolymers are not significantly different from each other and degree of polymerization found to be approximately 40 (Mn ~ 11880-13662). Although we added NDP monomer in excess but Degree of polymerization for second block did not exceeded than 46. This is because of the steric effect of azobenzene chromophore in the side chain [1]

Furthermore, after the introduction of the second block, there is slightly increase in the polydispersities. This could be due to the generation of new initiating species at longer reaction times, which can initiate polymerization at the later stages of the polymerization. Similar MWD broadening was also observed for other living radical polymerizations in solution, particularly at higher conversion.

Table 3.1 Feed ratios of all chemicals, conditions and expected molecular weights

Sample Code.	**[M]/[I]**	**[CuBr]/[I]**	**[L]/[I]**	**[$CuBr_2$]/[I]**	**Solvent (THF)**	**Temp**	**Time**	**$M_{n,\ theo}$**
TB 1	21.1	0.5	0.525	0.025	50%	60^{O}C	8 h	2560
TB 2	47.4	0.5	0.525	0.025	50%	60^{O}C	8 h	5760
TB 3	73.7	0.5	0.525	0.025	50%	60^{O}C	8 h	8960
TB 4	105.3	0.5	0.525	0.025	50%	60^{O}C	8 h	12800

Where

[M] = Moles of Monomer (t-butylacrylate)

[I] = Moles of Initiator (Ethyl-2-bromopropionate)

[L] = Moles of Ligand (PMDETA)

[CuBr] = Moles of Copper(I) Bromide

[$CuBr_2$] = Moles of Copper(II) Bromide

Solvent was taken on the basis of volume of monomer.

Theoretical molecular weights were calculated according to the formula [2]

$M_{n,\ theo} = 128([tBA]/[I] \times \text{conversion})$ Equation 3.1

3.3 DETERMINATION OF THE CHEMICAL STRUCTURE OF THE PREPARED BLOCK COPOLYMERS

The chemical structure of the prepared copolymers were characterized by 300 MHz ^{1}H NMR spectroscopy. The spectra of the copolymers showed features common to those expected to be present in the homopolymers of P(NDP) and P(t-BA). Peaks of the polymer found to be broad as compare to its monomer as shown in Figure 3.10. The assignments of the peaks were made by comparing the spectra of the copolymers with the homopolymers and others similar copolymers. The aliphatic region (1-2.5 ppm) shows the disappearance of sharp vinylic proton peaks of the monomer on polymerization, and disappearance of broad and overlapped resonances of backbone CH_2 and CH of the monomers repeat units in the copolymers to demonstrate copolymerization as shown in Figure 3.9.

The aromatic region (6.5-8.5 ppm) is simplified by the fact that it contains the peak present in the azo monomer repeat unit only. The chemical shift of ortho and meta protons of the benzene ring shift to lower field due to the presence of electron-withdrawing NO_2 group, and/or additional conjugation of the benzenoid ring. The CH_3 peak found to at 1.3 ppm and inagreemnt with published literature. The prepared polymer also exhibited the resonances of the chain end proton signal of EBriB at around 4.12 ppm.

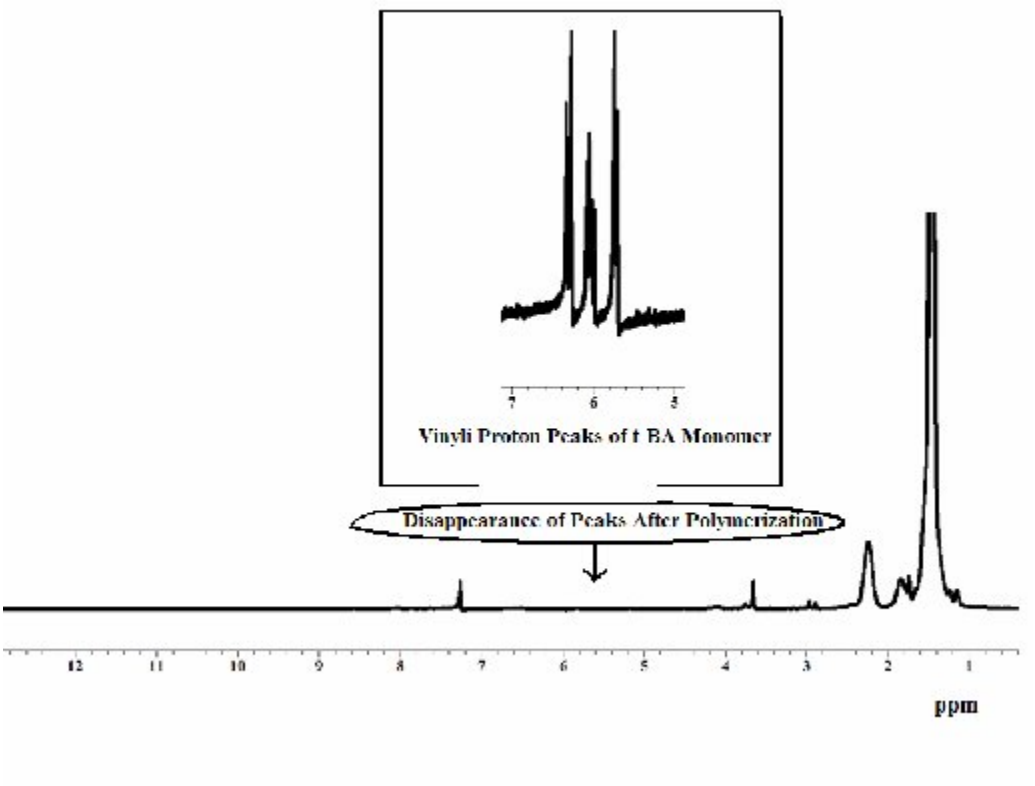

Figure 3.9 1H NMR spectrum of the prepared block of the macroinitiator, t-BA (P3). Inset shows the vinylic proton peaks of the monomer.

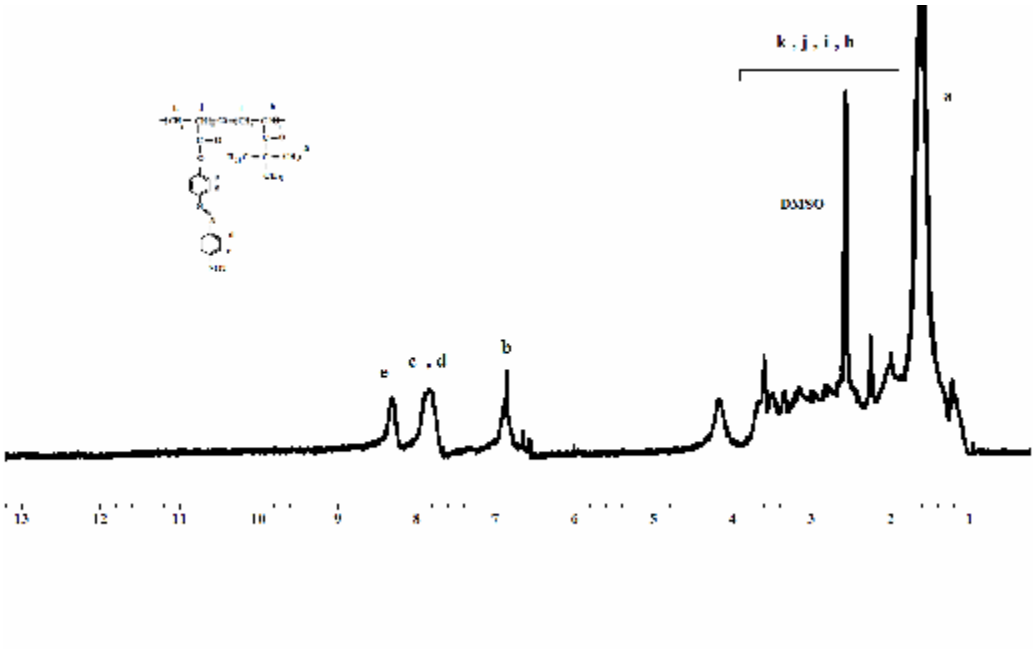

Figure 3.10 [1]H NMR spectrum of the prepared block of the P(t-BA-b-NDP) (P7).

3.4 MOLECULAR WEIGHT OF THE PREPARED BLOCK COPOLYMERS DETERMINED BY GEL PERMEATION CHROMATOGRAPHY (GPC)

Gel permeation chromatography (GPC) is the standard characterization tool to determine the molecular weight and molecular weight distribution of polymers. It operates under a size exclusion principle, i.e., the injected polymer solutions are separated based on their hydrodynamic volumes; species with larger hydrodynamic volumes—and hence larger sizes—elute at shorter times [3]. The basic principle of the technique is given in Figure.

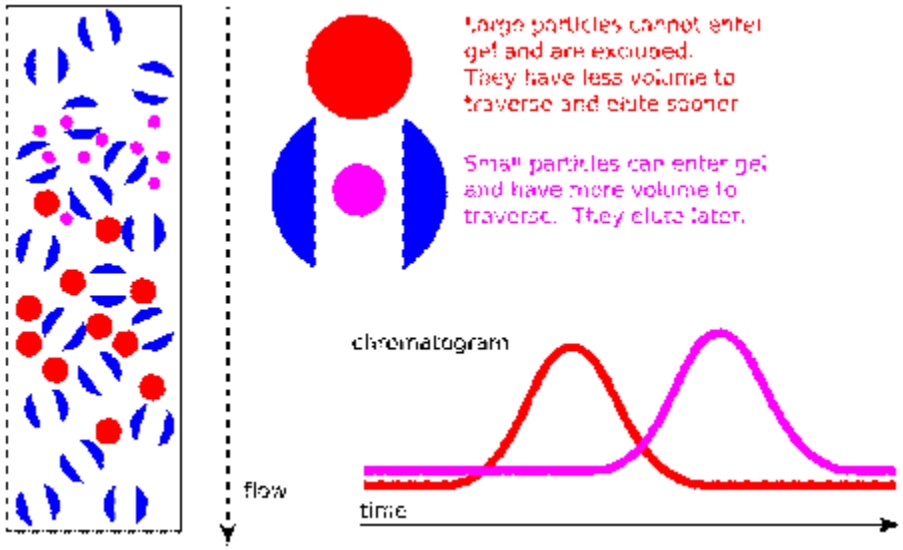

Figure 3.11 Schematic of the separation of the macromolecules

The hydrodynamic volume (*Vh*) of a polymer is directly proportional to the logarithm of its molecular weight, according to the following equation [3].

$$V_h = KM_v^{\,a+1}/2.5A = log(K/2.5A) + (a+1)log(M_v) \quad \text{Equation 3.2}$$

In Equation 3.2, *Mv* is the viscosity-average molecular weight, *A* is Avogadro's number, and *K* and *a* are the Mark-Houwink constants for a given polymer. These constants depend on the specific chemical structure of the polymer and its architecture, as well as the solvent and temperature employed during analysis [3]. The elution volume of

a polymer, which is equivalent to the elution time at a flow rate of 1 mL/min, is thus inversely proportional to the logarithm of its molecular weight.

In the current work, poly(t-butyl acrylate), P(t-BA) macroinitiator was used to polymerize the prepared azobenzene NDP monomer. P(t-BA)-Br terminated macroinitiator was first prepared and its degree of reactivity investigated by extension of polymerization of azobenzene NDP monomer. GPC measurements indicated that the P(t-BA)-Br terminated macroinitiator sample with extended molecular weight had a narrow molecular weight distribution with no observation residual macroinitiator and bimodality for all the four blocks copolymers. The controlled radical polymerization carried out in the current work confirmed the efficient extension polymerization using the P(t-BA)-Br terminated macroinitiator. The macroinitiator was then used to polymerize the azobenzene monomer, 2-propenoic acid, 4-[2-(4-nitrophenyl)diazenyl]phenyl ester (NDP monomer) to make the diblock. The representative GPC curves in Figure 1-3 indicate a successful initiation and growth of the second block. The elution time and/or volume of the P(t-BA) macroinitiator appeared later relative to that of the diblock copolymers. In other words, the GPC peak of the P(t-BA) macroinitiator moved to higher molecular weight region, and thereof indicate successful polymerization. The molecular weight data obtained from GPC analyses is summarized in Tables 3.2 and 3.3. Diblock copolymers with various contents (or volume fractions) of the azobenzene monomer can readily be obtained by controlling the conversion and/or the amount of azobenzene monomer added for the extension polymerization. In the current work, the block copolymers prepared have a polydispersity slightly higher than that of the P(t-BA) macroinitiator (1.25). This is not unusual, and has been reported in the literature for the case of block copolymers of azobenzene monomers [4].

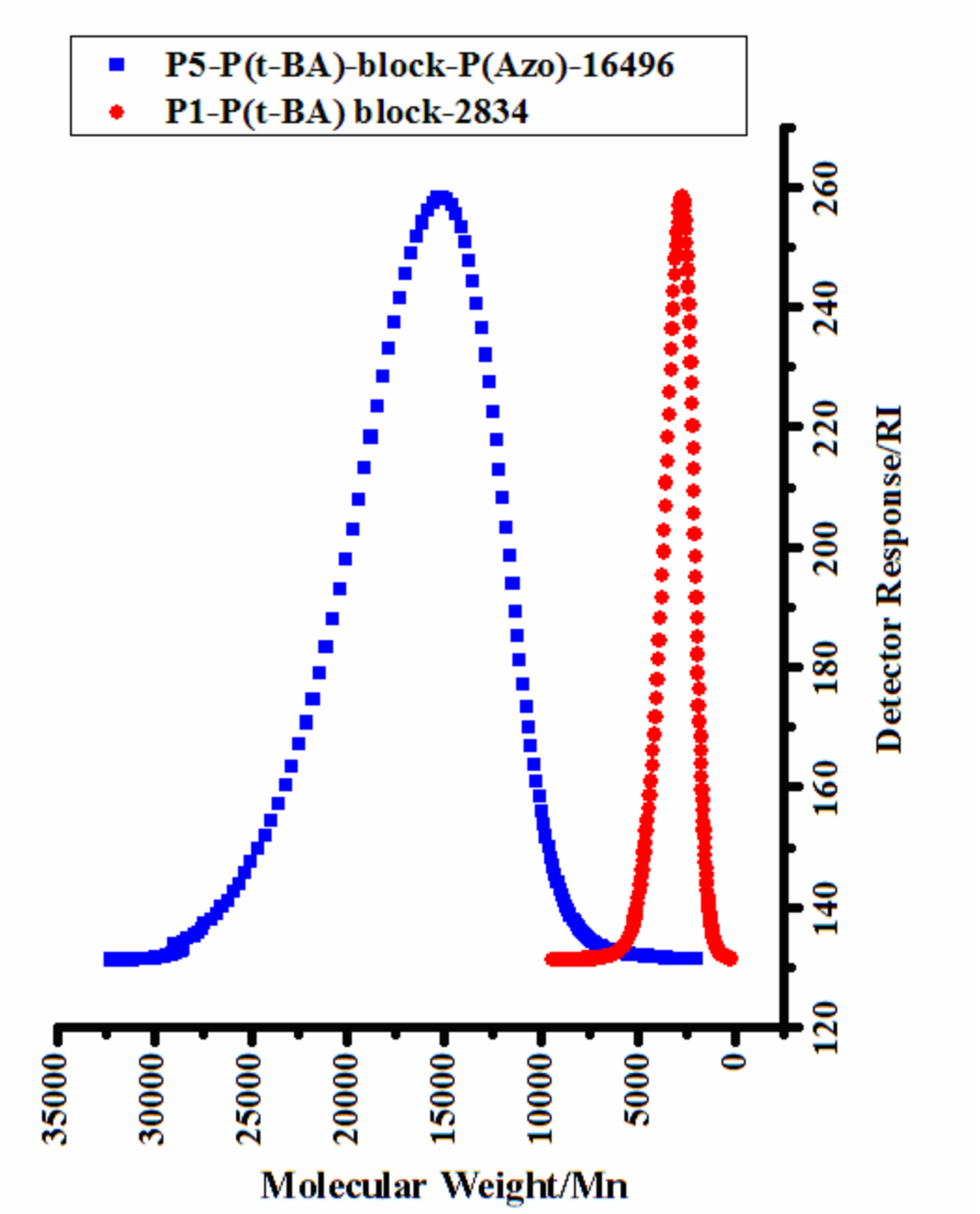

Figure 3.12 The GPC chromatograms exhibiting the molecular weight of polymer samples P1(Poly(tert-butylacrylate) and of P5 (Poly NDP). Block copolymer synthesized using P1 as macoinitiator.

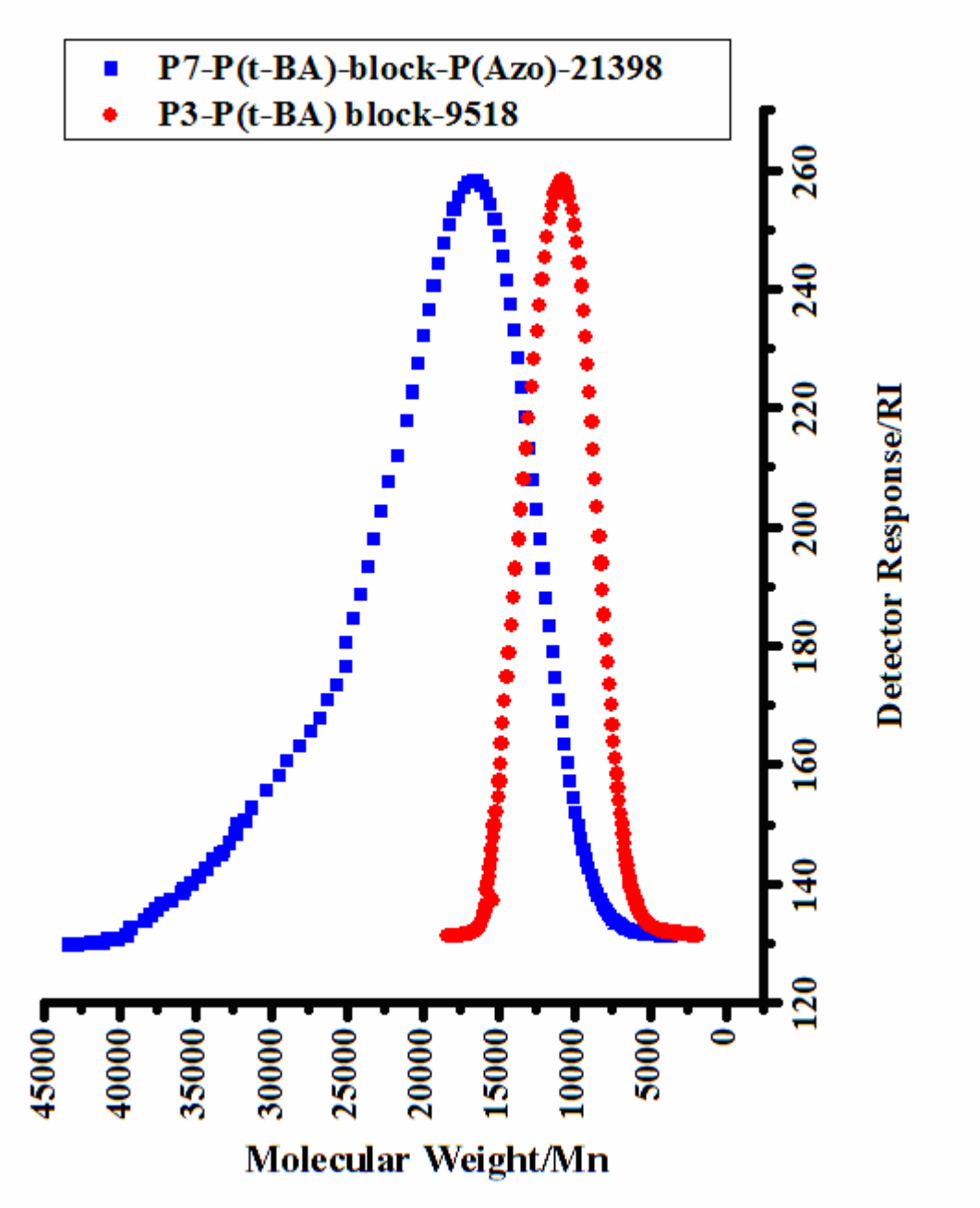

Figure 3.13 The GPC chromatograms exhibiting the molecular weight of polymer samples P3(Poly(tert-butylacrylate) and of P7 (Poly NDP). Block copolymer synthesized using P3 as macoinitiator.

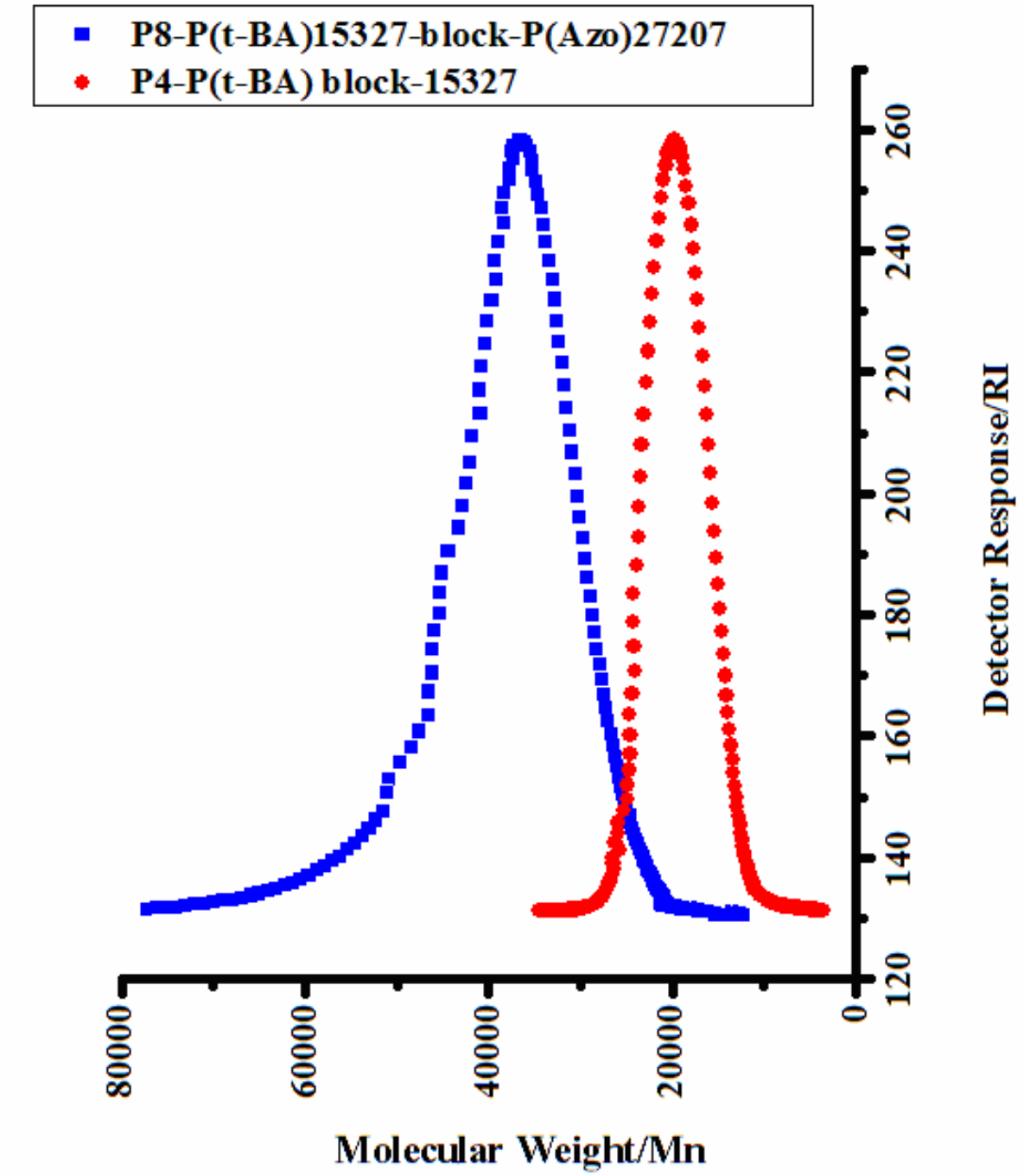

Figure 3.14 The GPC chromatograms exhibiting the molecular weight distributions of polymer samples P4 (Poly(tert-butylacrylate) macroinitiator and of P8 (Poly NDP). Block copolymer synthesized using P4 as macoinitiator.

Table 3.2 Sumary of GPC results for poly(tert-butylacrylate) macroinitiator

Polymer Sample Code	**Theoretical molecular weight ($M_{n, theo}$)**	**Targetted DP**	**Experimental Molecular Weight ($M_{n, exp}$)**	**Experimental DP**	**Experimental Molecular Weight ($M_{w, exp}$)**	**Mw/Mn**
P1	2560	20	2834	22	3373	1.19
P2	5760	45	5977	47	7172	1.20
P3	8960	70	9518	74	11136	1.17
P4	12800	100	15327	119	17319	1.13

Table 3.3 Summary of GPC results for poly(tert-butylacrylate)-block-poly(NDP)

Polymer Sample Code	**Experimental Molecular Weight of block copolymer ($M_{n, exp}$)**	**Experimental Molecular Weight of macroinitiator (Block 1) ($M_{n, exp}$)**	**Experimental Molecular Weight of (Block 2) ($M_{n, exp}$)**	**Experimental DP of Block 2**	**Experimental Molecular Weights of block copolymer ($M_{w, exp}$)**	**Mw/Mn**
P5	16496	2834	13662	46	20950	1.27
P6	19045	5977	13068	44	23425	1.23
P7	21398	9518	11880	40	26961	1.26
P8	27207	15327	11880	40	34009	1.25

It is evident from the GPC data that the obtained molecular weight of Poly(tert-butylacrylate) macroinitiator are very close to those theoretically targeted ones and found to be slightly higher. It seems that reactions have gone to almost complete completion.

Initial theoretical calculation were used since it was considered that the reaction may not go to completion. Theoretically targeted molecular weights were targeted by assuming 95% conversion of the tert-butylacrylate. The recalculations of the theoretically targeted molecular weights by assuming 100% conversion of tert-butylacrylate monomer give values which are even more closer to the experimentally obtained molecular weights. A comparison of the theoretically calculated molecular weight with 100% conversion to that of the experimentally obtained values is presented in Table 3.3.

Table 3.4 A comparison of Theoretical (assuming 100% monomer conversion) and Experimental Molecular Weights

Polymer Sample Codes.	**Theoretical molecular weight ($M_{n,\ theo}$)**	**Targetted DP**	**Experimental Molecular Weight ($M_{n,\ exp}$)**	**Experimental DP**
P1	2700	21	2834	22
P2	6067	47	5977	47
P3	9434	74	9518	74
P4	13478	105	15327	119

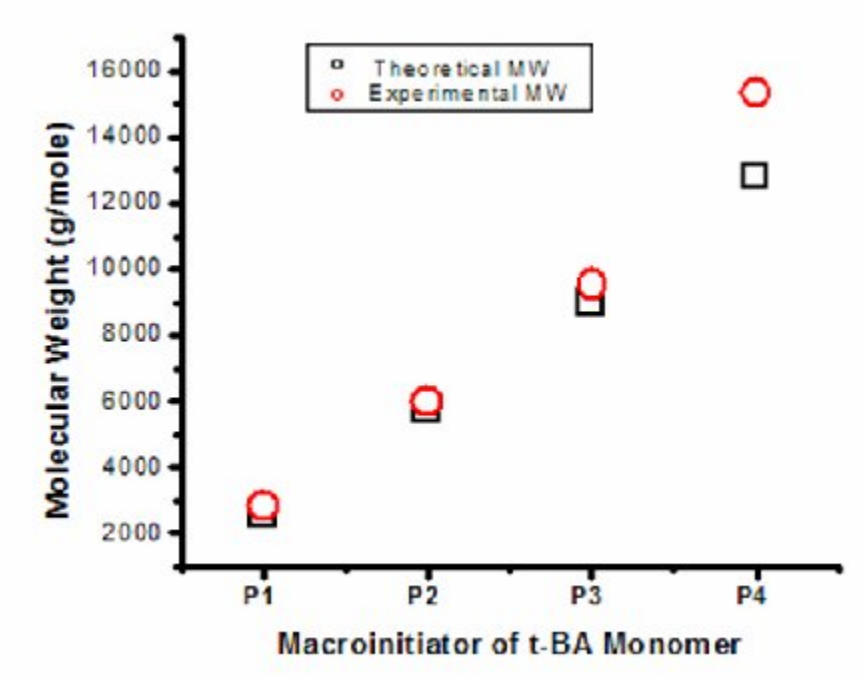

Figure 3.15 Graphical comparison of theoretical and experimental molecular weights

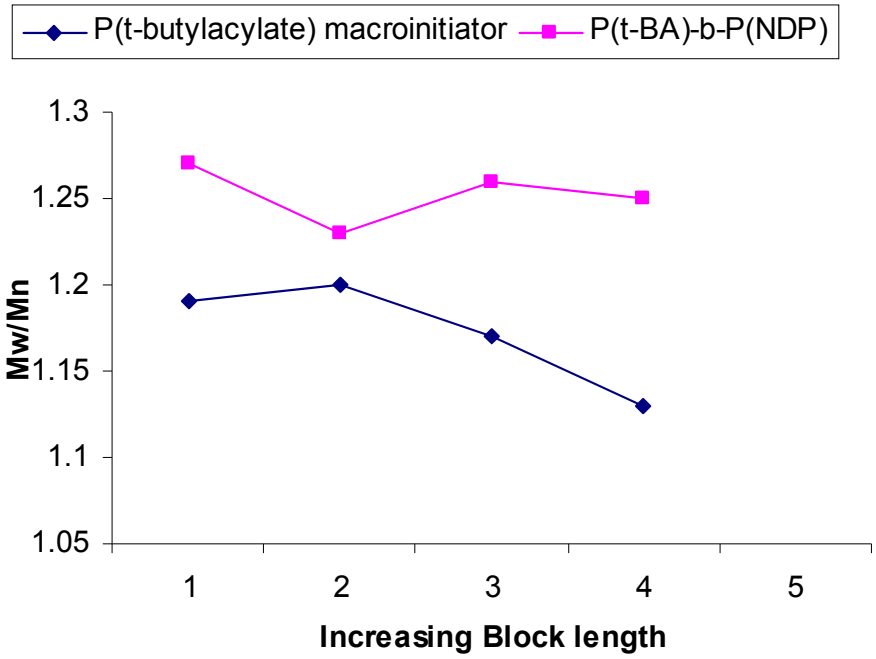

Figure 3.16 A comparison of Mw/Mn values for P(t-BA) macronitiator and P(t-BA)-b-P(NDP) block copolymer

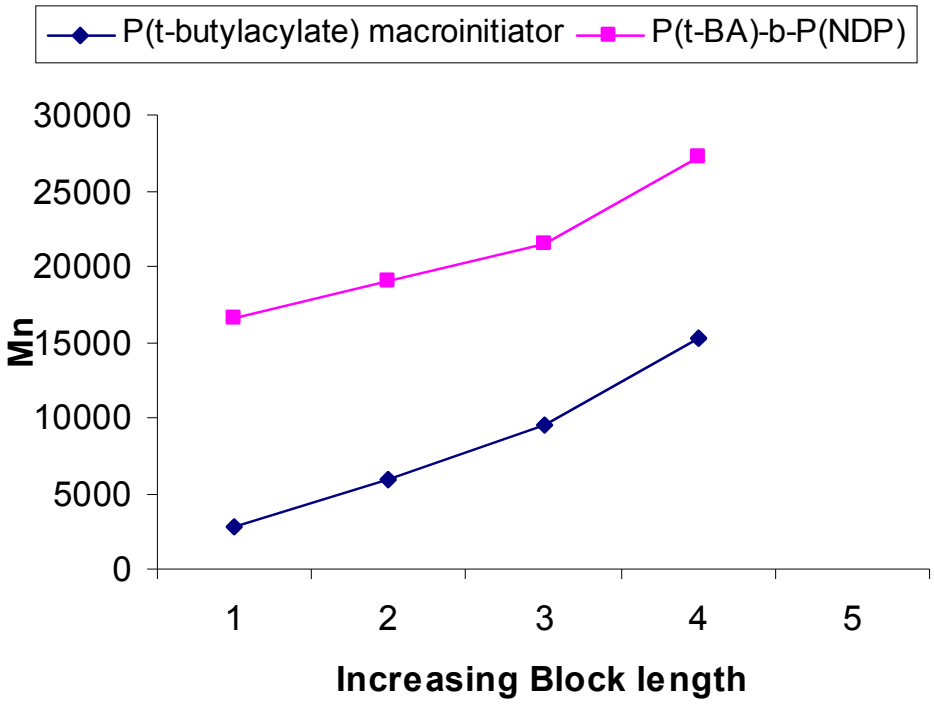

Figure 3.17 A comparison of Mn values for P(t-BA) macronitiator and P(t-BA)-b-P(NDP) block copolymer

3.5 CONCLUSIONS

In the current work novel functional polymeric materials were developed and used to synthesize Di-block copolymers. The developed polymeric materials possessed photo-responsive functionalities. The main conclusions of the research work are outlined below.

- A 4-[2-(4-nitrophenyl)diazenly]phenyl ester (NDP monomer) containing azo-chromophore was synthesized. IR and NMR spectra were used to confirm the sturucture of NDP monomer. UV-Vis absorption spectrum of the NDP monomer showed that λ_{max} is at 338nm shows transition of Geometric isomers. So it is expected that any polymers prepared from NDP monomer would be photo responsive.
- Four P(t-BA) macroinitiator blocks were prepared using ATRP and their molecular weights were determined using GPC. There was a good agreement between the theoretically calculated and experimentally determined Molecular weights of macroinitiators.
- These P(t-BA) macroinitiator blocks also found to have low M_w/M_n ratio (1.13-1.20) showing that the prepared blocks are of narrow molecular weight distribution.
- Four P(t-BA)-b-P(NDP) Di-block copolymers were synthesized using the prepared four P(t-BA) macroinitiator blocks by ATRP. The molecular weights of the Block copolymers show that the P(NDP) chain was grown only to certain extent (DP 40-46), which is mainly due to steric hindrance of the bulky phenyl groups.
- The structures of P(t-BA) macroinitiator and P(t-BA)-b-P(NDP) Di-block copolymers were confirmed using NMR specta.
- These Block copolymers are also found to have low M_w/M_n ratio (1.23-1.27), but higher than for macroinitiator blocks.
- Generally M_w/M_n ratio decreased on increasing molecular weights. Which is expected result.

3.6 FUTURE RECOMMENDATIONS

The main objective of current work was to synthesize photo-responsive Block copolymers. Good results have been obtained, both in terms of Molecular weights and M_w/M_n ratio. The developed experimental setup, techniques, procedures, reactions, and materials will provide useful platform to carry out future work to further advance the scientific and technological potential of these Block copolymers. Considering above, following are important future recommendations to continue the research work in the fascinating area of Drug delivery

- The prepared P(t-BA)-b-P(NDP) block copolymers could be hydrolyzed to produce amphiphilic P(AA)-b-P(NDP) block copolymers. These will be able to produce spectrum of morphologies in solutions. These polymers will also be pH responsive
- Studies of phase behaviour on such amphiphilic P(AA)-b-P(NDP) block copolymers can be performed, to out line possible morphologies which could be obtained using such polymers.
- It can also be studied that whether or not these produced morphologies are photo-reversible.
- An at the end based on the all above experimentation future of such photo-responsive block copolymers for use in Drug delivery systems can be outlined.

3.7 REFFERENCES

1. N. Li, J. Lu, Q. Xu, L. Wang, Optical Materials, 28, 1412 (2006)

2. K. A. Devis, K. Matyjaszewski, Macromolecules, 33, 4039 (2000)

3. Ciampolini, M.; Nardi, N. Inorg. Chem., 5, 41. (1966)

4. G. Wang, X. Tong, Y. Zhao, Macromolecules, 37, 8911 (2004)